JOC The Journal of Organic Chemistry

pubs.acs.org/joc Article

Evidence for the Formation of 1,2-Dioxetane as a High-Energy Intermediate and Possible Chemiexcitation Pathways in the Chemiluminescence of Lophine Peroxides

Andreia Boaro, Roberta Albino Reis, Carolina Santana Silva, Diêgo Ulysses Melo, Alexander Garreta Gonçalves Costa Pinto, and Fernando Heering Bartoloni*

Cite This: J. Org. Chem. 2021, 86, 6633−6647 Read Online

ACCESS | Metrics & More | Article Recommendations | Supporting Information

ABSTRACT: A kinetic study of the chemiluminescent (CL) reaction mechanism of lophine-derived hydroperoxides and silylperoxides induced by a base and fluoride, respectively, provided evidence for the formation of a 1,2-dioxetane as a high-energy intermediate (HEI) of this CL transformation. This was postulated using a linear Hammett relationship, consistent with the formation of negative charge on the transition state of HEI generation ($\rho > 1$). The decomposition of this HEI leads to chemiexcitation with overall low singlet excited state formation quantum yield (Φ_S from 1.1 to 14.5 × 10^{-5} E mol^{-1}); nonetheless, Φ_S = 1.20 × 10^{-3} E mol^{-1} was observed with both peroxides substituted with bromine. The use of electron-donating substituents increases chemiexcitation efficiency, while it also reduces the rate for both formation and decomposition of the HEI. Different possible pathways for HEI decomposition and chemiexcitation are discussed in light of literature data from the perspective of the substituent effect. This system could be explored in the future for analytical and labeling purposes or for biological oxidation through chemiexcitation.

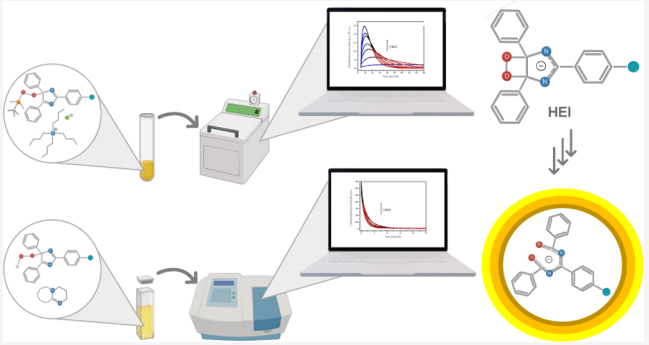

INTRODUCTION

More than 140 years ago, Radziszewski was the pioneer in the study of the chemiluminescence (CL) of lophine (i.e., 2,4,5-triphenyl-1*H*-imidazole, Scheme 1a, **L1**) in basic media and in the presence of oxygen.[1] Such transformation is historically important in the CL field for being used by Wiedemann in 1888 to define the term itself ("Das bei chemischen Prozessen auftretende Leuchten würde Chemilumineszenz genannt", i.e., the light emission observed during chemical processes must be called chemiluminescence).[2] Despite being the first-reported CL system, the mechanism of the lophine decomposition reaction, responsible for the generation of light, is not fully understood.[3] Detailed mechanistic studies of other CL transformations subsequently reported revealed that the light observed as a product of these reactions is generated from the exothermic decomposition of cyclic peroxide intermediates.[4−11]

To perform CL studies, a wide variety of lophine derivatives, substituted in the 2-phenyl group (Scheme 1a, **L1-6**) and in 4-phenyl and 5-phenyl (Scheme 1a, **L7-13**), were conveniently obtained by condensation of their corresponding benzaldehyde with benzil and NH_4OAc in acidic conditions.[3,12] The CL mechanism for **L1** and some of its derivatives (e.g., **L2**, **L7**, and **L8**, Scheme 1a) involves the reaction of lophine anion with oxygen, probably through a single-electron transfer (SET) process, generating a neutral lophine radical and a superoxide ion $O_2^{\bullet-}$ (Scheme 1b).[13−15] These radicals combine to produce a peroxyanion (**H**$^-$) that, after cyclization, results in a 1,2-dioxetane intermediate (Scheme 1c, **D**$^-$). The decomposition of cyclic peroxide **D**$^-$ in the so-called chemiexcitation step generates a deprotonated benzoylamidine derivative in the excited state (Scheme 1c, **B**$^{-}$*).[4,5,11,13−15] Finally, the last step consists in the fluorescence decay of **B**$^{-}$* to the ground state, generating light and **B**$^-$ as final reaction products (Scheme 1c).[4,9−11,13−15] This CL mechanism (Scheme 1b,c) shares some common aspects with bioluminescent systems comprising 1,2-dioxetanones as high-energy intermediates (HEIs).[4] For instance, evidence suggests that a SET reaction between O_2 and the enolates of the firefly[16−18] and cypridine[19] luciferins is involved in the formation of their corresponding peroxyanions.[4,5,11] These peroxyanions lead to the 1,2-

Received: February 19, 2021
Published: April 20, 2021

https://doi.org/10.1021/acs.joc.1c00230
J. Org. Chem. 2021, 86, 6633−6647

Scheme 1. Molecular Structure of Lophine (L), Hydroperoxide (H), and Silylperoxide (S) Derivatives (a); CL Reaction Mechanism for Lophine (L1) under Basic Condition and in the Presence of Oxygen (b,c); and for Hydroperoxides and Silylperoxides in the Presence of a Base and Fluoride Respectively (d,c)[a,3,13–15]

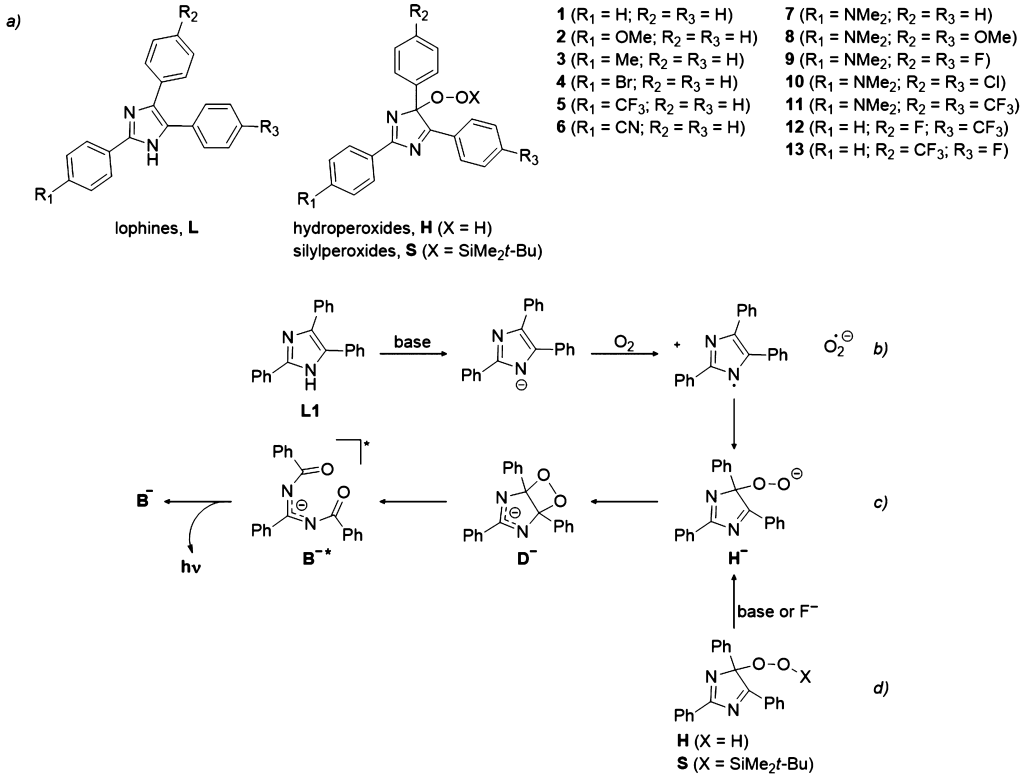

[a]HEI of this sequence is the 1,2-dioxetane anion (D^-).

dioxetanone HEIs necessary for generation of excited states.[4,5,11]

Isolated hydroperoxides (e.g., **H1**, **H2**, and **H7**, Scheme 1a), prepared from their corresponding lophines by photooxygenation, are also chemiluminescent in basic conditions (KOH in EtOH).[13] The CL reaction of these hydroperoxides generates benzoylamidines emitting at the same wavelength of the CL reaction of lophines.[13] It is postulated that in basic conditions, **H** is deprotonated to the peroxyanion H^- (Scheme 1d), and CL arises from the decomposition of the common intermediate D^- (Scheme 1c).[13,20] However, no direct evidence for the formation of this 1,2-dioxetane as HEI has been reported. Kimura et al., studying the CL of **H7-11** (Scheme 1a) with KOH in MeOH/CH_2Cl_2 1:5, commented that H^- cyclization to produce D^- (Scheme 1c) could be the rate-determining step of the CL reaction.[21] Lu et al. studied the isomeric silylperoxides (*R*)-**S12** and (*R*)-**S13** (Scheme 1a), whose CL was triggered by addition of fluoride tetrabutylammonium (TBAF) in $CHCl_3$ or acetone.[3] The lower CL quantum yield (Φ_{CL}) in acetone for (*R*)-**S12** when compared to (*R*)-**S13** was attributed to the involvement of a partially cyclic transition state (TS) at the chemiexcitation step.[3] In $CHCl_3$, CL efficiencies were equal within experimental errors, suggesting that 1,2-dioxetane D^- plays a main role in the formation of excited states in this solvent.[3] To access the occurrence of D^- as a HEI on this CL system, in this work, we have conducted a thorough kinetic study on the decomposition of **H1-5** and **S1-6** (Scheme 1a). Substitution only at the 2-phenyl ring was intentional to observe the substituent effect on peroxides directly related to Radziszewski's **L1** chemiluminescence. In addition, we propose that the electronic nature of substituents seems to play a role in determining the multiplicity of the excited state, resulting from chemiexcitation.

RESULTS AND DISCUSSION

Peroxide Preparation and Photophysical Characterization. Six lophine derivatives (**L1–6**, Scheme 1a) were obtained from the condensation of their corresponding para-substituted benzaldehyde with benzil and NH_4OAc in glacial acetic acid (Scheme 2a).[3,12,22] Our research group has been

Scheme 2. Preparation of Lophines L1–6 (a), Their Corresponding Hydroperoxides H1–6 (b), and Silylperoxides S1–6 (c), with R_1 = H (1), OMe (2), Me (3), Br (4), CF_3 (5), and CN (6)[a]

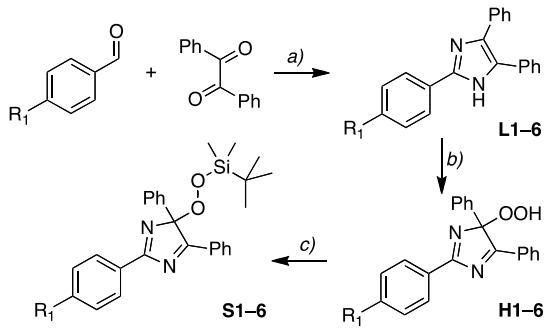

[a]Methods: (a) NH_4OAc in glacial HOAc; (b) $^1O_2$ in CH_2Cl_2/ACN 5:1; (c) TBDMSCl and IMI-H (cat.) in CH_2Cl_2.

https://doi.org/10.1021/acs.joc.1c00230
J. Org. Chem. 2021, 86, 6633–6647

Table 1. Photophysical Properties for the Studied Lophines (L), Hydroperoxides (H), Silylperoxides (S), and Benzoylamidines (B): Maximum Absorption Wavelength (λ_{abs}), Molar Extinction Coefficient (ε), Maximum Fluorescence Wavelength (λ_{FL}), Fluorescence Quantum Yield (Φ_{FL}), Stokes Shift ($\Delta\lambda$), and Maximum Chemiluminescence Wavelength of the CL Reaction (λ_{CL}).[a]

	λ_{abs}[b] (nm)	ε[c] (L mol^{-1} cm^{-1})	λ_{FL}[b] (nm)	Φ_{FL}[d]	$\Delta\lambda$[e] (cm^{-1})	λ_{CL}[f] (nm)
L1	306	27,600 ± 300	383	0.42 ± 0.02	6750	
L2	302	29,000 ± 200	394	0.37 ± 0.01	7730	
L3	306	26,800 ± 100	388	0.41 ± 0.01	6910	
L4	314	30,200 ± 200	385	(1.41 ± 0.05) × 10^{-2}	5870	
L5	320	25,900 ± 600	402	0.70 ± 0.03	6370	
L6	342	24,520 ± 20	431	0.74 ± 0.03	6040	
H1	278	20,700 ± 100	384	(1.9 ± 0.1) × 10^{-3}	9930	522
H2	302	24,960 ± 60	394	(7.6 ± 0.2) × 10^{-3}	7730	527
H3	284	24,630 ± 80	389	(3.8 ± 0.1) × 10^{-3}	9500	528
H4	282	25,600 ± 100	384	(6.8 ± 0.7) × 10^{-4}	9420	516
H5	249	16,300 ± 70	402	(8.9 ± 0.4) × 10^{-3}	15,300	516
S1	277	21,500 ± 200	380	(7.0 ± 0.4) × 10^{-4}	9800	530
S2	301	17,150 ± 60	394	(8.2 ± 0.7) × 10^{-4}	7840	520
S3	282	23,200 ± 80	386	(5.5 ± 0.3) × 10^{-4}	9550	520
S4	281	25,460 ± 90	360	(3.1 ± 0.5) × 10^{-4}	7810	519
S5	249	17,540 ± 40	401	(7.8 ± 0.3) × 10^{-4}	15,220	520
S6	267	29,830 ± 30	431	(4.3 ± 0.4) × 10^{-3}	14,250	502
B1[g]	238		384	(7.3 ± 0.2) × 10^{-2}	15,970	
B2[g]	274		394	(4.9 ± 0.1) × 10^{-2}	11,115	
B3[g]	237		387	(5.8 ± 0.2) × 10^{-2}	16,350	
B4[g]	256		385	(3.4 ± 0.6) × 10^{-3}	13,090	
B5[g]	242		437	0.21 ± 0.01	18,440	
B6[g]	260		475	0.25 ± 0.02	17,410	

[a]Mean value ±standard deviation for at least three replicas. [b]Obtained at 25 °C in ACN for **L1−6**, **H1−5**, and **S1−6**, and in ACN/THF 17:3 v/v for **B1−6**. [c]Determined as the angular coefficient of λ_{abs} versus concentration linear plots with the intercept set as zero ($r > 0.99$). [d]Determined with 2,5-diphenyloxazole (Φ_{FL} = 0.70) in EtOAc as the relative standard;[32] for low-intensity emissions, **H2** was used as the secondary standard. [e]Calculated as the difference between λ_{abs} and λ_{FL} with both previously converted to cm^{-1}. [f]Determined for the CL reaction of **H1−5** (1.0 mmol L^{-1}) or **S1−6** (0.1 mmol L^{-1}) in the presence of 1,8-diazabicyclo(5.4.0)undec-7-ene (DBU, 10 mmol L^{-1}) or TBAF fluoride (1.0 mmol L^{-1}), respectively, both in ACN. [g]For **B1−6**, parameters λ_{abs}, λ_{FL}, and $\Delta\lambda$ were determined directly from **S1−6** solutions following the addition of TBAF.

using this method for the preparation of substituted imidazoles for different applications.[23−25] After purification, these lophine derivatives were converted to their hydroperoxides (**H1−6**, Scheme 1a) by reacting with singlet oxygen generated by photosensitization with methylene blue (Scheme 2b).[3] This method is equivalent to the one used for the synthesis of alkyl-1,2-dioxetanes from olefins.[26,27] Finally, silylperoxides (**S1−6**, Scheme 1a) were prepared by protection of the **H1−6** hydroperoxyl group with *tert*-butyldimethylsilyl chloride (TBDMSCl, Scheme 2c). Details for the preparation and characterization of the compounds are given in the Experimental Section.

The photophysical characterization of all derivatives of lophine, hydroperoxide (except for **H6** due to its unsuccessful purification), silylperoxide, and benzoylamidine was performed in acetonitrile (ACN) to evaluate and compare their light emission properties (Table 1). As expected, all lophines **L1−6** presented high fluorescent quantum yield ($\Phi_{FL} > 0.3$, Table 1).[24,25,28] The derivative substituted with bromine **L4**, with $\Phi_{FL} \approx 0.01$, is an exception, probably a result of the heavy atom effect, increasing intersystem crossing and generating nonemissive triplet states.[29−31] The lophine derivatives containing the withdrawing substituents CF_3 and CN (**L5** and **L6**, respectively) showed a bathochromic shift in their maximum absorption (λ_{abs}) and fluorescence (λ_{FL}) wavelengths and higher Φ_{FL} compared to other lophine derivatives (Table 1 and Figure S1a,b). The presence of such withdrawing substituents increases conjugation in the structures of **L5** and **L6**, resulting in an approximation of their fundamental and excited states that favors electron transitions.[23−25,28,29]

The peroxides **H1−5** and **S1−6** exhibited blue-shifted λ_{abs} (Figure S1c,e), and no difference in λ_{FL} compared to their corresponding lophines (Table 1 and Figure S1b,d,f). **H1−5** showed lower Φ_{FL} (in the 10^{-3} range) than **L1−5** due to the presence of the sp^3-hybridized carbon-4 bonded to the peroxidic group (Table 1). With this sp^3 atom, the imidazole ring is no longer fully conjugated, and the phenyl rings become significantly twisted and out-of-plane when compared to lophines.[33] Such molecules become less rigid, leading to an increase in thermal deactivation of excited states, decreasing the Φ_{FL} of these hydroperoxides.[29]

As seen for **L1−6**, electron-withdrawing substituents also shifted λ_{FL} of **H1−5** and **S1−6** to longer wavelengths (Table 1 and Figure S1d,f) due to increased conjugation. The peroxides **S1−6** displayed lower Φ_{FL} values (in the 10^{-4} range) when compared to their corresponding hydroperoxides (Table 1). Such lower Φ_{FL} values can be attributed to an increased number of vibrational modes associated to the organosilicon group, which augments thermal deactivation of excited states.[29] CL spectra of **H1−5** and **S1−6** after addition of DBU (1,8-diazabicyclo(5.4.0)undec-7-ene) and TBAF (TBAF fluoride), respectively, provided values of maximum CL emission wavelengths (i.e., λ_{CL}, Figure S1g,h) that correspond to the emission from the excited state of deprotonated benzoylami-

https://doi.org/10.1021/acs.joc.1c00230
J. Org. Chem. 2021, 86, 6633−6647

dines (B^-, Scheme 1c). The conjugate base B^- is the emitter of the CL reaction of lophine derivatives, as originally noted in previous reports.[13−15] The longer λ_{CL} values (in the 502−530 nm range, Table 1) are expected, since all B^- derivatives are fully conjugated species due to their anionic nature.[3,13,16]

Absorption and fluorescence spectra were recorded after the CL reaction between **S1−6** with TBAF in order to obtain the values of λ_{abs} and λ_{FL} for all final CL reaction products (**B1−6**, Table 1 and Figure S1i,j). The benzoylamidines **B1−6** exhibited lower values of λ_{FL} compared to the λ_{CL} of the reaction (Table 1 and Figure S1j,h), indicating that the emitter B^- acquired a proton from the reaction medium after ground-state formation, generating the less conjugated protonated benzoylamidine (**B**, Scheme 3). In other words, B^- is the conjugate base of a photoacid, but it is generated directly on the excited state from the CL pathway.[13−15] The benzoylamidines **B1−6** possess relatively high Stokes shift values ($\Delta\lambda$ > 11,000 cm^{-1}, Table 1) when compared to other studied compounds, which is usually treated as evidence of excited-state intramolecular proton transfer (ESIPT).[24,33−35] The observed fluorescence of **B1−6** can occur from the deactivation of the excited state of a keto-like tautomer and an enol-like tautomer (enol-**B**, Scheme 3), the latter generated with the intramolecular movement of the N-bonded proton after species **B** absorbs an excitation photon. Since there is no report in the literature concerning ESIPT with benzoylamidines as substrates, this could be explored in the future, particularly regarding the relevance of ESIPT with nitrogen as proton donor.[36] The benzoylamidine containing bromine as substituent (**B4**) presented the lowest Φ_{FL}, as also noted for **L4** (Table 1), in agreement with the generation of nonemissive triplet excited states due to the heavy atom effect.[29−31]

Scheme 3. Acid−Base Equilibrium Involving the Deprotonated Benzoylamidine (B^-) and Its Conjugated Acid (B) after Light Emission from the CL Reaction and Possibility of Keto−Enol Tautomerization from B to an Enol-Like Species (Enol-B)

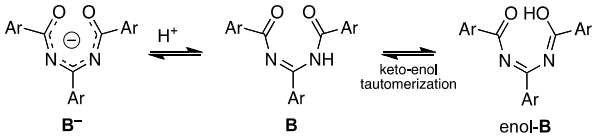

Chemiluminescence Kinetics. *General Remarks.* We studied the kinetics of the CL reaction of **S1−6** with TBAF in ACN/tetrahydrofuran (THF) 17:3 v/v and of **H1−6** with DBU in ACN using the peroxides under the pseudo-first-order condition. Kinetics were studied following light intensity over time, and the registered profiles consisted of a rapid CL increase upon addition of TBAF or DBU to a solution of **S1−6** or **H1−5**, respectively, followed by a slower exponential decay (Figure 1). Results obtained with **S1−6** will be discussed prior to **H1−5**.

Kinetics with Silylperoxides Using a Luminometer. CL measurements with **S1−6** were performed in a commercial test tube luminometer, with TBAF stock solutions added to the tube already containing **S1−6** (1.27 μmol L^{-1}) through a set of automatic injectors. CL intensity−time profiles (Figure 1) were very reproducible, and the observed rate constants k_{obs}^1 and k_{obs}^2, as well as the maximum emission intensity (I_{max}) were obtained fitting the fall and rise in intensity using eqs 1 and 2, respectively, for different concentrations of TBAF (Tables S1−S6).

$$I(t) = I_{max}(e^{(-k_{obs}^1 t)}) \quad (1)$$

$$I(t) = I_{max}(1 - e^{(k_{obs}^2 t)}) \quad (2)$$

Observed rate constants k_{obs}^1 and k_{obs}^2 are associated with the first and second steps of the CL mechanism (Scheme 4) from the perspective that 1,2-dioxetane D^- is the intermediate of a complex consecutive reaction.[37] Other CL reactions have analogous intensity−time profiles, where the rise (k_{obs}^2) and

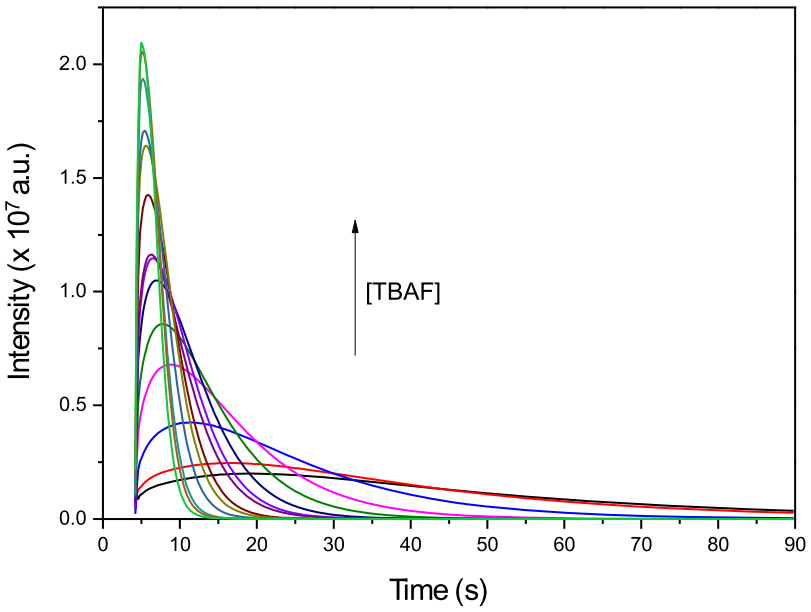

Figure 1. Examples of CL intensity−time profiles obtained with **S4** (1.27 μmol L^{-1}) upon addition of TBAF (at 15 different concentrations, from 0.052 to 0.210 mmol L^{-1}) in ACN/THF 17:3 v/v at 25 °C, using a commercial tube luminometer. TBAF was added after 4 s of initiating data acquisition.

https://doi.org/10.1021/acs.joc.1c00230
J. Org. Chem. 2021, 86, 6633−6647

Scheme 4. Stepwise Mechanism for the CL of S1−6, with Deprotection of the Silyl Group by Fluoride Generating H^- (Step 1) and Cyclization to the HEI D^- (Step 2)[a]

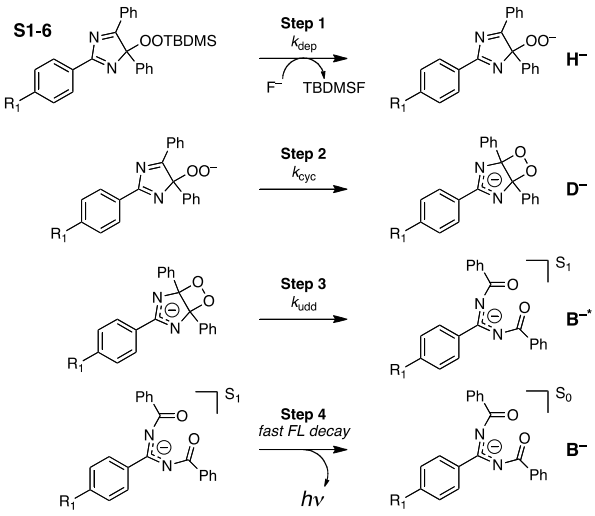

[a]Decomposition of D^- generates B^-* (step 3) that decays to its B^- ground state (step 4) in a process that is always faster than the previous ones.

fall (k_{obs}^1) rate constants were attributed to the second and first steps, respectively, of an intricate mechanistic sequence.[25,32,38−42] The bimolecular rate constant for the deprotection of **S1−6** by fluoride (k_{dep}, Scheme 4, step 1) was determined from a linear correlation between k_{obs}^1 and the concentration of TBAF (Figure S2 and Table 2). Although the formation of D^- from H^- (Scheme 4, step 2) is a unimolecular process that does not involve fluoride, the concentration of H^- at a given time depends on the previous step.[29,37] Therefore, the rate constant for the cyclization process and generation of D^- (k_{cyc}, Scheme 4, step 2) was obtained through the linear dependence between k_{obs}^2 values and the concentration of TBAF for **S1−5** (Figure S3 and Table 2).

Table 2. Rate Constants for the Deprotection of S1−6 by Fluoride Generating H^- (k_{dep}) and for the Cyclization of H^- Generating the 1,2-Dioxetane HEI D^- (k_{cyc}), Within the Studied CL Reaction Mechanism (Scheme 4)

peroxide	R_1	σ_p[a]	k_{dep} ($\times 10^3$ L mol^{-1} s^{-1})	k_{cyc} ($\times 10^4$ L mol^{-1} s^{-1})
S2	OMe	−0.27	1.30 ± 0.05	0.76 ± 0.03
S3	Me	−0.17	2.13 ± 0.04	1.49 ± 0.03
S1	H	0	2.38 ± 0.02	1.88 ± 0.03
S4	Br	+0.23	4.20 ± 0.10	5.70 ± 0.09
S5	CF_3	+0.54	5.80 ± 0.30	9.70 ± 0.60
S6	CN	+0.66	5.10 ± 0.06	

[a]Values for the Hammett substituent constant (σ_p) taken from ref 43.

Derivatives with electron-withdrawing substituents (**S4−6**) showed higher values for both rate constants, k_{dep} and k_{cyc} (Table 2). Such results indicate the generation of negative charge in the TSs of both reaction steps (Scheme 4, steps 1 and 2, Scheme 5). This is quantitatively assessed through linear free-energy relationships using the Hammett substituent constant (σ_p),[44] obtaining the reaction constants ρ = +0.7 and +1.5 for plots with k_{dep} and k_{cyc}, respectively (Figure 2).

Scheme 5. TSs Involved in the (a) Deprotection Reaction of S1−6 by Fluoride (Scheme 4, Step 1) and (b) Generation of the 1,2-Dioxetane HEI in the CL of S1−6 (Scheme 4, Step 2)

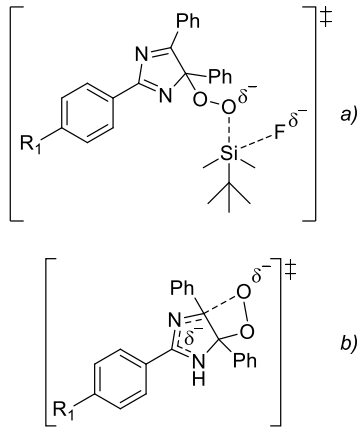

These positive ρ values are consistent with negative charge being developed in the TS of both stages (Scheme 4, steps 1 and 2, Scheme 5).[43] The value of ρ < 1 for k_{dep} shows that the deprotection reaction (Scheme 4, step 1) is less sensitive to substituents than the hydrolysis reaction of benzoic acid methyl esters.[43] In fact, the partial negative charge generated in the peroxidic oxygen of the TS (Scheme 5a) is relatively far from the substituent, not being so susceptible to its electronic effect. On the other hand, for the reaction of D^- formation (Scheme 4, step 2), a negative charge is being created at the heterocycle directly bonded to the substituted aromatic ring, involving both nitrogen atoms in its delocalization (Scheme 5b). Substituents attached to the arylimidazolic system have a pronounced electronic effect on the stability of the TS of this step (Scheme 4, step 2, Scheme 5b). The magnitude of ρ value obtained for the cyclization reaction (+1.5) is a direct kinetic evidence for the formation of a 1,2-dioxetane as a HEI in the decomposition of this class of peroxides, related to Radziszewski's CL oxidation of **L1** (Scheme 1b,c).

A linear dependence between k_{obs}^2 and TBAF concentration can be observed but not within the entire range of studied fluoride concentration (Figure S3). For **S1** and **S3**, the values of k_{obs}^2 tend to stabilize, reaching a maximum value of 2.1 and 1.7 s^{-1}, respectively, at [TBAF] > 0.15 mmol L^{-1} (Tables S1 and S3 and Figure S3). For **S2**, this trend is not so clear; although, for this derivative, the k_{obs}^2 value reaches an average of 1.8 s^{-1} also above 1.5 mmol L^{-1} of TBAF (Table S2 and Figure S3). For **S4** and **S5**, the k_{obs}^2 value did not have a significant increase above 0.1 mmol L^{-1} of TBAF, reaching maximum values around 3.5 and 5.5 s^{-1}, respectively (Tables S4 and S5 and Figure S3). These maximum values for k_{obs}^2 are observed at TBAF concentrations in which the decomposition of D^- (Scheme 4, step 3) becomes rate-limiting when compared to its formation (Scheme 4, step 2). Thus, these are the unimolecular rate constants associated with the 1,2-dioxetane decomposition (k_{udd}). The unimolecular decomposition of D^-, involving O−O and C−C cleavage,[4,5,11] is faster for derivatives with electron-withdrawing substituents (k_{udd} = 5.5 s^{-1}, **D5**$^-$) than the donor (k_{udd} = 1.7 s^{-1}, **D3**$^-$). The lack of systematic dependence of k_{obs}^2 with [TBAF] for **S6** may be related to the strong electron-withdrawing −CN group, with rate constants being obtained close to the maximum limit established by the unimolecular decomposition of the

https://doi.org/10.1021/acs.joc.1c00230
J. Org. Chem. 2021, 86, 6633−6647

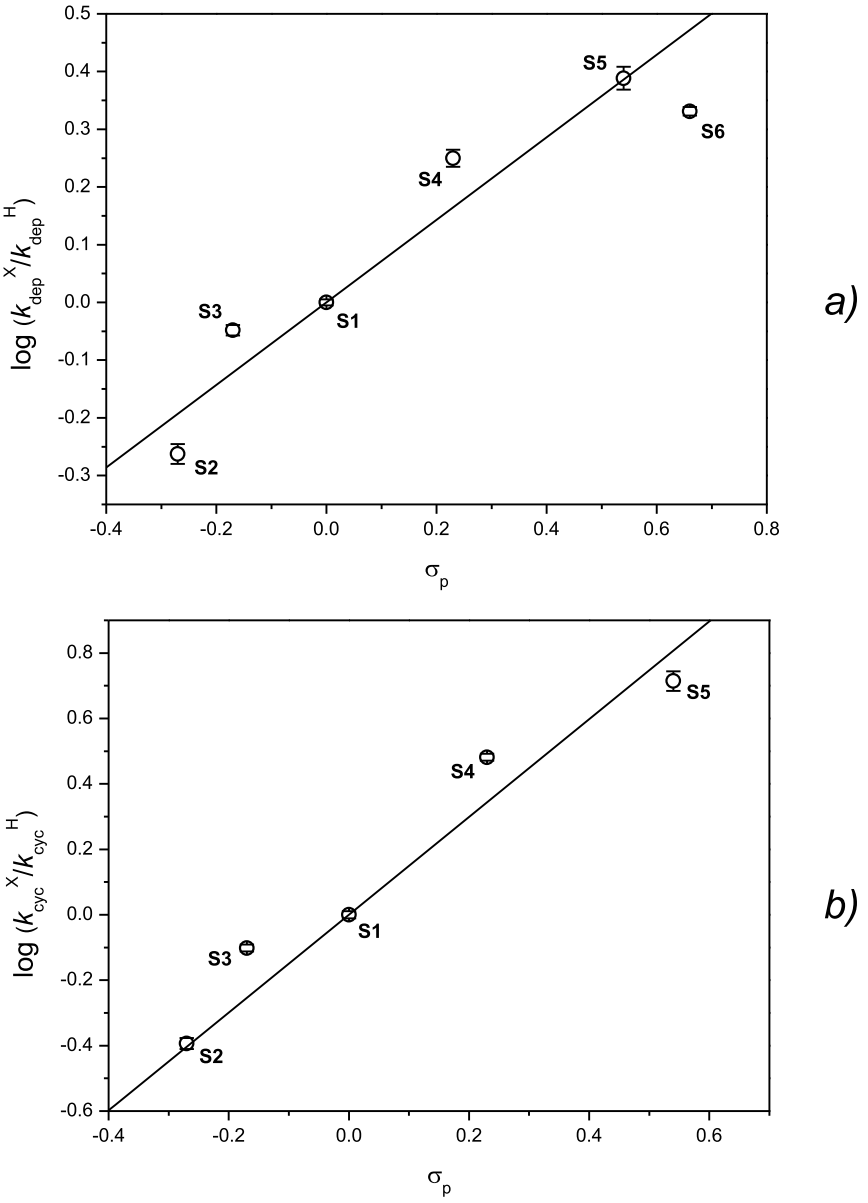

Figure 2. Linear free-energy relationship with (a) k_{dep} and (b) k_{cyc} using the Hammett constant for para substitutions (σ_p). From the angular coefficients, reaction constants ρ = +0.7 ± 0.1 and +1.5 ± 0.3 were determined for plots with k_{dep} and k_{cyc}, respectively, both with fair linear relationships (r > 0.9). Derivative **S6** was not included in the correlation.

corresponding **D6**$^-$ (k_{udd} *ca.* 4 and 9 s^{-1}, Table S6 and Figure S3).

Kinetics with Silylperoxides Using a Fluorescence Spectrophotometer. We have also performed kinetic measurements using a fluorescence spectrophotometer, with a fluorescence quartz cuvette already containing a solution of **S1**, **S2**, and **S4** (0.025 mmol L^{-1}) in ACN, equipped with a magnetic stirrer. Data acquisition was initiated after addition of a TBAF stock solution in THF using a glass microsyringe. The obtained intensity−time profiles (data not shown) are similar to those registered with the luminometer (Figure 1); however, only emission decay can be observed. Kinetics with the fluorescence spectrophotometer is not as reproducible as with the luminometer, and the used silylperoxide concentration must be 20 times higher due to the inherent lower sensibility of the equipment.

CL decay−time profiles obtained with the fluorescence spectrophotometer were fitted to determine k_{obs}^{1} (eq 1), for different TBAF concentrations (between 0.25 and 2.00 mmol L^{-1}), using peroxides **S1**, **S2**, and **S4** (Table S7). From the linear dependence between such a decay rate constant and TBAF concentration (Figure S4), values for k_{dep} were obtained as (1.25 ± 0.04) × 10^3, (2.74 ± 0.07) × 10^3, and (3.4 ± 0.1) × 10^3 L mol^{-1} s^{-1} for **S2**, **S1**, and **S4**, respectively. These bimolecular k_{dep} values are significantly comparable to those obtained with the luminometer (Table 2). Although the deprotection step can be kinetically observed when a fluorescence spectrophotometer is utilized, the faster cyclization reaction is not accessible with this experimental setup. The formation of the 1,2-dioxetane HEI was only observed kinetically with the luminometer, as described in the previous section.

The linear dependence between k_{obs}^{1} and [TBAF], for **S1**, **S2**, and **S4** (Figure S4), reaches constant values at high fluoride concentrations, as previously observed for the dependence between k_{obs}^{2} and [TBAF] obtained using the

https://doi.org/10.1021/acs.joc.1c00230
J. Org. Chem. 2021, 86, 6633−6647

luminometer (Figure S3). At [TBAF] > 1.4 mmol L^{-1}, the decomposition reaction of $\mathbf{D}^-$ (Scheme 4, step 3) becomes rate-limiting. This is observed for k_{obs}^1 only when using the spectrophotometer since TBAF (i.e., the excess reagent) is present at concentrations that are at least 1 order of magnitude higher than those used in the luminometer. The k_{udd} values obtained using the spectrophotometer (3.3, 2.1, and 4.0 s^{-1} for **S1**, **S2**, and **S4**, respectively) are in excellent agreement with the k_{udd} values determined using the luminometer (2.1, 1.8, and 3.5 s^{-1} for **S1**, **S2**, and **S4**, respectively). Thus, all these results, obtained by kinetic assays performed on the luminometer and fluorescence spectrophotometer, support the proposed overall mechanism for the CL decomposition of **S1−6** (Scheme 4).

Kinetics with Hydroperoxides Using a Fluorescence Spectrophotometer. CL measurements with **H1−5** were performed using a commercial fluorescence spectrophotometer using a fluorescence quartz cuvette already containing a solution of **H1−5** (0.20 mmol L^{-1}) in ACN, equipped with a magnetic stirrer. Data acquisition was initiated after addition of a stock solution of DBU in ACN using a glass microsyringe. Other bases were used to trigger CL emission, such as pyridine (pK_{aH} = 5.25),[45] imidazole (pK_{aH} = 6.95),[46] 4-dimethylaminopyridine (pK_{aH} = 9.20),[46] triethylamine (pK_{aH} = 10.75),[46] and pyrrolidine (pK_{aH} = 11.27);[47] however, only DBU (pK_{aH} = 13.5)[48] afforded reproducible intensity−time profiles (Figure S5).

Emission decay kinetic profiles obtained for **H1−5** at DBU concentrations between 1.0 and 10.0 mmol L^{-1} were fitted to determine the k_{obs}^1 values (eq 1 and Table S8). A linear dependence between k_{obs}^1 and [DBU] was observed until 4.0 mmol L^{-1} of DBU for all hydroperoxide derivatives **H1−5** (Figure S6). From these linear fittings, a bimolecular rate constant was determined (Table 3, k_{DBU}), being at least 2 orders of magnitude lower than k_{dep} and k_{cyc} for the reaction of **S1−6** with fluoride (Table 2). Indeed, these results are in accordance with the empirical observation of longer reaction times for CL kinetics with peroxides **H1−5** than with **S1−6**.

Table 3. Rate Constants for the Bimolecular DBU-Induced CL of H1-5 (k_{DBU}) and for the Unimolecular 1,2-Dioxetane Decomposition (k_{udd})

peroxide	R_1	σ_p[a]	k_{DBU} (× 10^2 L mol^{-1} s^{-1})	k_{udd} (s^{-1})
H2	OMe	−0.27	0.26 ± 0.02	0.25 ± 0.01
H3	Me	−0.17	0.40 ± 0.01	0.34 ± 0.01
H1	H	0	0.77 ± 0.03	0.54 ± 0.03
H4	Br	+0.23	1.64 ± 0.06	1.21 ± 0.01
H5	CF_3	+0.54	3.06 ± 0.08	1.68 ± 0.04

[a]Values for the Hammett substituent constant (σ_p) taken from ref 43.

The reaction constant ρ = +1.2 ± 0.1 was obtained through a Hammett plot with k_{DBU} (Figure 3a).[43] The positive signal and magnitude (>1) of such a ρ value indicates that a negative charge is being generated on the TS and is susceptible to the electronic nature of substituents, as with k_{cyc} for the cyclization of intermediate $\mathbf{H}^-$ generated from **S1−6** (Scheme 5b).[43] This result suggests general base catalysis by DBU, with the abstraction of a proton coupled to cyclization and 1,2-dioxetane formation (Scheme 6). Compared to the general mechanism proposed for the CL of **S1−6** (Scheme 4), for **H1−5**, the reaction pathway would be slightly different with steps 1 and 2 combined on a single concerted process. In water, the pK_a of organic hydroperoxides have been shown to vary from 8 to 12, depending on their structure;[49] nonetheless, DBU seems to be basic enough to promote deprotonation of **H1−5** as long as it occurs concomitant to peroxide cyclization.

Above 4 mmol L^{-1} of DBU, the values of k_{obs}^1 remain constant (Table S8 and Figure S6), as it was observed with **S1**, **S2**, and **S4** in the experiments conducted on the fluorescence spectrophotometer (Figure S4). The unimolecular rate constant for the decomposition of the HEI, k_{udd}, of the CL reaction of **H1−5** was also observed (Table 3), as well as for **S1−6** in the experiments performed in the luminometer. k_{udd} values for **H1−5** (Table 3) are lower than those determined for **S1−5** (2.1, 1.8, 1.7, 3.5, and 5.5 s^{-1}, respectively), but the systems are not exactly equivalent, particularly with respect to solvation (**S1−6** in ACN/THF 17:3 v/v and **H1−5** in ACN). Nevertheless, k_{udd} is associated with the decomposition of the same HEI, 1,2-dioxetane $\mathbf{D}^-$, regardless of the peroxide used to generate it (Schemes 5b and 6). Although only the chemiexcitation process is being represented here, the conversion of $\mathbf{D}^-$ to $\mathbf{B}^-$, involving O−O and C−C cleavage (Scheme 4, steps 3 and 4),[4,5,11] may or may not occur with the formation of excited states (i.e., $\mathbf{B}^-$*). Therefore, k_{udd} cannot be interpreted solely as the chemiexcitation rate constant; as a matter of fact, it incorporates any other process associated with the decomposition of the HEI.

The effect of substituent nature on k_{udd} is clear, with electron-withdrawing groups leading to higher rate constant values (Table 3); this was observed for the **S1−6** system, although not with such a significant trend (see previous sections). The reaction constant ρ = +1.3 ± 0.1 was obtained from the Hammett plot for k_{udd} (Figure 3b), indicating that a negative charge is associated with the TS and that this system is more sensitive to substituents than benzoic acid derivatives.[43] This information is going to be used in the interpretation of excitation yields and in the rationalization of the chemiexcitation mechanism discussed in the following sections.

Chemiluminescence and Excited State Formation Yields. Intensity-time profiles obtained for **S1−6** and **H1−5** at different concentrations of TBAF and DBU, respectively, were integrated and converted to chemiluminescence quantum yields (Φ_{CL}); see Experimental Section for details. Φ_{CL} was independent of the fluoride or base concentration, and mean values of this yield were obtained for each peroxide derivative (Table 4). Therefore, regardless of the concentration of the used excess reagent (i.e., TBAF or DBU), the light emission efficiency depended exclusively on the amount of limiting peroxide available (i.e., **S1−6** or **H1−5**). This is a relevant information, considering that higher concentrations of fluoride or base could have catalyzed the decomposition of peroxides through alternate "dark" routes. The peroxyoxalate reaction is an example of a CL system that has its emission efficiency decreased drastically with increasing concentration of base due to "dark" HEI decomposition.[4,41,42,50]

Considering all six peroxides **S1−6**, the average for Φ_{CL} is (3.7 ± 0.7) × 10^{-6} E mol^{-1} (Table 4). This value is in the same order of magnitude than the Φ_{CL} for the chemiluminescence of (*R*)-**S12** and (*R*)-**S13** (Scheme 1a) in acetone triggered by TBAF.[3] White and Harding reported that upon treatment with potassium superoxide in EtOH, the Φ_{CL} for **L1** is 10^{-6} to 10^{-7} E mol^{-1}, while for **L8** (Scheme 1a), the Φ_{CL} is10^{-3} to 10^{-4} E mol^{-1}.[13] The CL reaction of silylperoxides

https://doi.org/10.1021/acs.joc.1c00230
J. Org. Chem. 2021, 86, 6633−6647

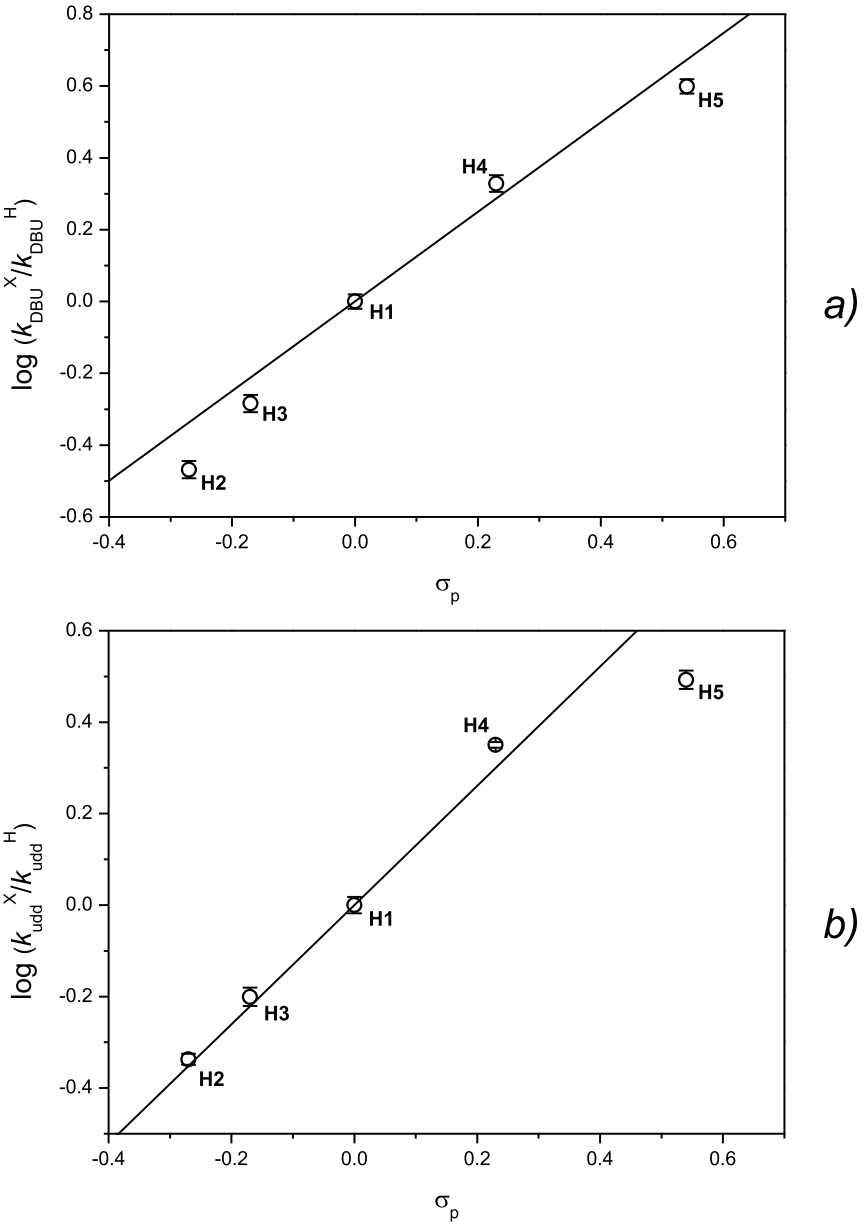

Figure 3. Linear free-energy relationship for (a) k_{DBU} and (b) k_{udd} using the Hammett constant for para substitutions (σ_p). From the angular coefficients, reaction constants ρ = +1.2 ± 0.1 and +1.3 ± 0.1 were determined for plots with k_{DBU} and k_{udd}, respectively, both with fair linear relationships (r > 0.9).

Scheme 6. TS Involved in the Formation of the 1,2-Dioxetane HEI on the CL Reaction Mechanism of H1−5 With DBU

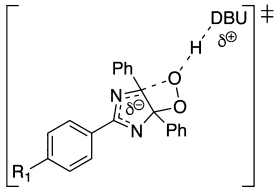

triggered by fluoride has low efficiency when compared to other light-emitting systems.[4,5,25,32]

The singlet excited-state formation quantum yield (Φ_S) can be determined by correcting Φ_{CL} by the fluorescence quantum yield (Φ_{FL}) of the emitter $\mathbf{B}^-$; see Experimental Section for details. The Φ_S value is a direct measure of the chemiexcitation process efficiency (Scheme 4, steps 3 and 4), and this yield goes from 1.1 × 10^{-5} to 7.8 × 10^{-5} E mol^{-1} for **S1−3**, **S5**, and **S6** (Table 4). Φ_S values for **H1−3** and **H5** are close to those determined for their corresponding silylperoxides **S1−3** and **S5** (Table 4). Although there is no absolute correlation between the chemiexcitation efficiency and the electronic nature of the substituents, it was observed that derivatives containing electron-donor substituents showed higher Φ_S values. This was also observed by White and Harding,[13] and Kimura et al. consciously used a $-NMe_2$ substituent on the 2-phenyl group at **H7−11** (Scheme 1a) to achieve higher Φ_{CL} and Φ_S values.[21] The yield for singlet state generation for **S1−6** and **H1−5** is low, compared to other CL systems that possess Φ_S close to unity.[5,51,52]

Nonetheless, peroxides **S4** and **H4** presented Φ_S = 1.20 × 10^{-3} E mol^{-1}, 2 orders of magnitude higher when compared to peroxides containing electron-withdrawing substituents (Table

https://doi.org/10.1021/acs.joc.1c00230
J. Org. Chem. 2021, 86, 6633−6647

Table 4. Chemiluminescence Quantum Yield (Φ_{CL}) and Singlet Excited State Formation Quantum Yield (Φ_S) for the CL Decomposition Reaction of S1−6 and H1−5 Induced by Fluoride and DBU, Respectively

peroxide	R_1	Φ_{CL} ($\times 10^{-6}$ E mol^{-1})	Φ_S ($\times 10^{-5}$ E mol^{-1})
S2[a]	OMe	3.8 ± 0.2	7.8 ± 0.4
S3[a]	Me	3.9 ± 0.2	6.7 ± 0.4
S1[a]	H	4.7 ± 0.3	6.4 ± 0.4
S4[a]	Br	4.2 ± 0.7	120 ± 20
S5[a]	CF_3	2.9 ± 0.6	1.4 ± 0.3
S6[a]	CN	2.8 ± 0.3	1.1 ± 0.5
H2[b]	OMe	7.1 ± 0.2	14.5 ± 0.4
H3[b]	Me	5.7 ± 0.3	9.8 ± 0.5
H1[b]	H	8.5 ± 0.7	11.6 ± 0.9
H4[b]	Br	3.9 ± 0.6	120 ± 20
H5[b]	CF_3	3.6 ± 0.7	1.7 ± 0.3

[a]For reactions with [**S1−6**] = 1.27 μmol L^{-1} and different TBAF concentrations (see Tables S1−S6 for details). [b]For reactions with [**H1−5**] = 0.2 mmol L^{-1} and DBU concentrations from 1.0 to 10.0 mmol L^{-1}.

4). This may be understood as evidence for the formation of additional singlet excited states (i.e., S_1) from triplet states with the bromine substituent favoring reverse intersystem crossing (RISC).[29,53,54] It is known that lower-energy triplet states of π/π^* nature can be produced on the decomposition of aryl-substituted 1,2-dioxetanes generating the corresponding carbonyl residues, in addition to the generally observed triplet n/π^* states.[11,55−58] In our case, a possible lower π/π^* triplet state of the aryl-substituted $\mathbf{B}^{-*}$ emitter containing a bromine group could enable RISC to the S_1 and explain the increased Φ_S for **S4** and **H4**. This hypothesis suggests that the yield of generation of overall triplet states (Φ_T) is higher than Φ_S for both peroxidic systems (**S1−6** and **H1−5**); however, in the absence of a bromine substituent, RISC cannot occur and an increase in singlet excites states is not evident. Recently, it has been shown that triplet excited states are likely the emitters in the solid-state thermochemiluminescence of **H1**,[59] supporting our proposition that in solution, (nonemissive) triplet states could also be generated. However, our results are not conclusive, and additional experimental and theoretical data are required to verify the occurrence of triplet excited states on the decomposition of **S1−6** and **H1−5**. Moreover, the possible

Scheme 7. Possible Mechanisms for the Chemiexcitation Step During the Decomposition of a 1,2-Dioxetane HEI in the Lophine Peroxide CL Reaction from Kimura et al.,[21] Lu et al.,[3] and This Work[a]

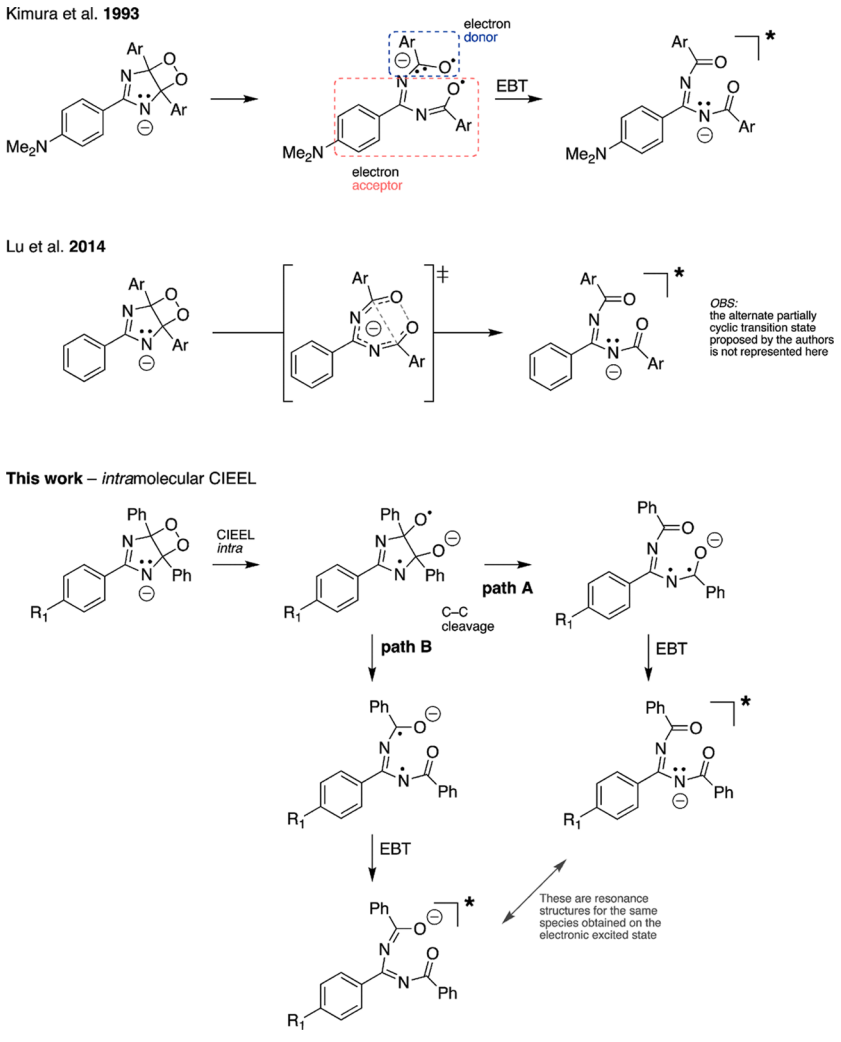

[a]Asterisk at the top of the benzoylamidine species indicates an electronic excited state, whether it is singlet or triplet.

https://doi.org/10.1021/acs.joc.1c00230
J. Org. Chem. 2021, 86, 6633−6647

occurrence of RISC with **S4** and **H4** should also be further investigated.

Possible Chemiexcitation Mechanisms for the Decomposition of Lophine Peroxides. Regardless of the originating peroxide, **S1−6** or **H1−5**, the corresponding 1,2-dioxetane $\mathbf{D}^-$ is generated as the HEI. Considering our results discussed above, we can assume that the $\mathbf{D}^-$ decomposition follows the chemiexcitation mechanism proposed for the thermal decomposition of 1,2-dioxetanes and 1,2-dioxetanones.[4,5,60,61] Such mechanism have shown $\Phi_S < 10^{-2}$ E mol^{-1}, where the peroxidic bond cleavage enters a biradical region associated with triplet states.[4,5,59,60] This hypothesis could be better supported by future computational simulation studies. For a while, our strongest evidence is the increased Φ_S value observed for the bromine substituted **S4** and **H4**, when compared to other derivatives. For the uncatalyzed decomposition of 1,2-dioxetanes, it has been determined experimentally that excited carbonyl residues are formed with Φ_T *ca.* 0.5 E mol^{-1}.[4,11,62,63] The determination of the actual Φ_T values for the CL of **S1−6** and **H1−5** could be performed, but an adequate experimental approach has not yet been proposed. If the role of triplet states is confirmed, this should be considered in the future use of lophine silylperoxides as sensors for biological systems.[4] The conjugation of a lophine silylperoxide to a peptide or protein would allow the use of this class of peroxides as CL probes for labeling biomolecules.[64] While singlet excited states are important for analytical and labeling purposes,[4,64] triplet states generated *in situ* could be used for assessing biological oxidation through chemiexcitation instead of light absorption,[65] also known as "dark" photochemistry.

Kimura et al.[21] postulated that the HEI produced from **H7−11** decomposes through a [2 + 2] cycloelimination reaction, generating a biradical anion intermediate (Scheme 7). They proposed that excited states are formed by an intramolecular electron reorganization (or electron back-transfer, EBT) between donor and acceptor moieties of the molecule, leading to excited states.[21] With **H7−11**, the formation of a biradical anion intermediate prior to excited states was explicitly addressed.[21] Such a view is a bit different from the fully concerted [2 + 2] cycloelimination reaction that directly produces triplet states in the thermal decomposition of 1,2-dioxetanes.[4,11,59−63]

Lu et al.,[3] when discussing that a partially cyclic TS may be involved on the chemiexcitation process for CL with (*R*)-**S12** and (*R*)-**S13**, considered that bond cleavage and formation should occur simultaneously for the generation of excited states (Scheme 7) in a view that is more equivalent to the fully concerted thermal decomposition of 1,2-dioxetanes.[4,11,59−63] Their conclusion[3] is supported by our observation that triplet states are generated in higher yields than singlet states, as seen by the increased Φ_S value observed for the bromine induced RISC (Table 4).

One possibility that has not been formally considered so far is that chemiexcitation on the decomposition of $\mathbf{D}^-$ may happen via the intramolecular chemically initiated electron exchange luminescence (CIEEL) mechanism.[66−68] The intramolecular CIEEL mechanism is used to rationalize the induced decomposition of aryl-1,2-dioxetanes that have high Φ_S values,[4,5] reported as 0.6 E mol^{-1}[69,70] and even 1.0 E mol^{-1}.[71] In our proposition (Scheme 7), an intramolecular electron transfer induces O−O bond cleavage and generation of a biradical anion. Then, C−C bond cleavage can occur through two different paths (Scheme 7A,B), leading to new biradical anions that have the formal negative charge and the unpaired electron in different carbonyl groups. The EBT generates two different resonance structures for the same species in the excited state, regardless of the path that is taking place (Scheme 7). Regarding the hydroperoxides **H7−11** studied by Kimura et al.,[21] the presence of the strong electron-donating group $-NMe_2$ on the 2-phenyl ring may promote chemiexcitation mainly through the intramolecular CIEEL sequence, justifying the Φ_S between 0.11 and 0.79 E mol^{-1} reported by these authors.

With respect to our results, the Φ_S values for the silylperoxides and hydroperoxides with electron-donating substituents are higher than the ones with electron-withdrawing groups (Table 4). For example, with **S2** and its methoxy group, Φ_S is up to 5.5 and 7-times higher than the values for **S5** and **S6**, with their corresponding CF_3 and CN substituents. With **H2** and **H5**, comprising the OMe and CN substituents, Φ_S is 8.5-times higher for the former. This suggests that the CIEEL contribution to the overall decomposition of $\mathbf{D}^-$ increases with increased electron-donating ability of the substituent at the 2-phenyl ring, which in turn facilitates intramolecular electron transfer and O−O bond cleavage (Scheme 7).[4,11,69−71] Thus, our reasoning suggests that with **S1−6** and **H1−5**, the transformation would still occur mainly through a mechanism that resembles the thermal decomposition of alkyl-1,2-dioxetanes and 1,2-dioxetanones[4,5,11,59−63] but with the CIEEL sequence becoming slightly more relevant with electron-donating substituents at the 2-phenyl ring.

In this intramolecular CIEEL landscape, the difference between the chemiexcitation efficiencies for hydro- and silylperoxides bearing the same substituent (e.g., **H2** and **S2**) must be accounted for. Consistently, the Φ_S value for the silylperoxide is smaller than the one for the corresponding hydroperoxide (Table 4), even if the difference is not that significant for yields of this nature.[7,11] For a given substituent, the same HEI cyclic peroxide $\mathbf{D}^-$ is going to be generated, regardless of the starting peroxide (Schemes 5b and 6). One must remember that the solvating media for the CL transformation with **S1−6** was ACN/THF 17:3 v/v, while pure ACN was used with **H1−5**. Adam, Matsumoto, and Trofimov proposed that an increase in viscosity prevents C−C bond rotation, frictionally reducing ground-state formation of molecules and increasing chemiexcitation yields.[72] This dependence of Φ_S in viscosity has been debated more recently,[8,73,74] and it seems that chemiexcitation in the intramolecular system is compromised when conformational changes compete with the concerted EBT and C−C bond cleavage.[8] Thus, it is hypothesized that the observed differences in Φ_S values for hydro- and silylperoxides bearing the same substituent are actually related to the influence of a solvent-cage effect on the overall EBT efficiency[8] and not to the starting peroxide structure. Our interpretation could be better supported by additional experimental data, employing different mixtures of benzene/diphenylmethane as reaction media.[8,72] This binary solvent system allows for different viscosities without significantly affecting the solvent reorganization energy and has been successfully applied for both intramolecular[8,72] and intermolecular CIEEL systems.[73,74]

So far, for the rationalization of the CL reaction with peroxides derived from lophine derivatives, it is suggested that electron-withdrawing groups on the 2-phenyl ring increase the rate of formation of the 1,2-dioxetane HEI (Schemes 5b and

https://doi.org/10.1021/acs.joc.1c00230
J. Org. Chem. 2021, 86, 6633−6647

6). They also increase the rate of decomposition of the cyclic peroxide (conversion of $\mathbf{D}^-$ to $\mathbf{B}^-$, Scheme 4, step 3), which may occur through a concerted [2 + 2] cycloelimination step (Scheme 7). However, with increasing electron-donating ability of the substituent, the intramolecular CIEEL pathway (Scheme 7) becomes more evident. As discussed above, this is not observed kinetically but can be inferred based on the increased singlet excited-state quantum yields of derivatives with electron-donating groups (Table 4). The CIEEL mechanism was originally devised to explain the efficient formation of excited states in intermolecular systems;[66−68] however, further investigation[52,75] showed that this process is actually orders of magnitudes less efficient than previously reported. An alternative charge transfer induced luminescence mechanism[4,75−77] was proposed to rationalize the low efficiency of singlet excited state formation in intermolecular systems, although the CIEEL mechanism is still successful to explain the high chemiexcitation efficiency for many intramolecular systems.[4−7,52,69−71] Nevertheless, research studies have reported that electron and/or charge transfer and back-transfer are not necessarily involved on the highly efficient imidazopyrazinone-based chemi-/bioluminescence.[78−80] For this system, efficient chemiexcitation occurs when the decomposition of the 1,2-dioxetanone HEI is delayed, allowing the molecule to spend more time on a region of the potential energy surface where ground and excited states are degenerated, thus augmenting the possibility of transition between electronic states.[79,80] Concerning our results with **S1−6** and **H1−5**, we have observed that electron-donating substituents decrease the rate of decomposition of $\mathbf{B}^-$ to $\mathbf{D}^-$ involved in the chemiexcitation step (Scheme 4, step 3). Thus, alternatively to the CIEEL process, this rationale could explain the increased Φ_S values observed for electron-donating substituted hydro- and silylperoxides (Table 4). As it can be seen, there are plenty of opportunities to continue the investigation on the CL decomposition of peroxides derived from lophine derivatives, both experimentally and theoretically.

CONCLUSIONS

In summary, we have provided evidence that a 1,2-dioxetane $\mathbf{D}^-$ is generated as a HEI on the CL of lophines hydroperoxides (Scheme 6) and silylperoxides (Scheme 5b). At high fluoride or DBU concentrations, the unimolecular decomposition of this HEI becomes rate-limiting. Electron-withdrawing groups increase both the rate of 1,2-dioxetane $\mathbf{D}^-$ formation and decomposition, while the latter may occur through a concerted [2 + 2] cycloelimination. With stronger electron-donating groups at the 2-phenyl ring, a higher contribution of the intramolecular CIEEL mechanism at the decomposition of $\mathbf{D}^-$ may be responsible for the increased Φ_S values that were observed, although there are other possible mechanistic alternatives. Nevertheless, additional experiments and theoretical simulations are required to rationalize excited state formation with peroxides derived from lophine and its derivatives. The Φ_S = 1.20 × 10^{-3} E mol^{-1} observed with bromine-substituted derivatives **S4** and **H4** may be possibly related to the presence of triplet states and RISC, although this is still under investigation. If indeed confirmed, the possibility of modulation in excited-state multiplicity could be explored in the future, whether there is interest in light emission or "dark" photochemistry induced by the decomposition of hydroperoxides or silylperoxides.

EXPERIMENTAL SECTION

General Section. All chemicals used in this work were purchased from commercial sources as analytical-grade reagents and used without further purification. Deionized water was obtained through a Milli-Q Millipore purifying system (conductivity 18.2 MΩ cm). Quartz cuvettes (Hellma, QS Suprasil) had a volume of 3.0 mL and an optical path of 10.00 mm, with two polished sides for absorption and four sides for fluorescence or chemiluminescence assays. Small sample volumes (μL) were transferred using Hamilton glass microsyringes. All the reported CL parameters were obtained as mean value ± standard deviation for at least three replicas at the same experimental condition. The purity of the peroxides used in kinetic measurements (over 97% in mass) was determined by iodometry using the method of spectrophotometric quantification of I_3^- reported elsewhere.[50−52,81]

Equipment. ^{1}H and ^{13}C NMR spectra were recorded at 25 °C using a 500 MHz Varian or 300 MHz Bruker DPX spectrometer. Elemental analyses were carried out on a Thermo Scientific Flash EA 1112 analyzer. For UV−vis absorption and fluorescence emission assays, Varian Cary 60 and Varian Cary Eclipse spectrophotometers were used, respectively; both equipment cell holders were maintained at 25 °C using a Varian Cary PCB 1500 system. Chemiluminescence measurements were performed using the spectrophotometer mentioned above with the emission monochromator set at the mirror position and with the excitation lamp shut off. For fast CL kinetic measurements, a Berthold Sirius single-tube luminometer with a set of automatic injectors was used.

Lophine L1−6 Preparation. Based on the method of Benisvy et al.,[22] as previously reported by our group,[23−25] for the preparation of lophine derivatives, a 50 mL round-bottom flask was charged with 2.7 g (12.9 mmol) of benzil, 7.4 g (96 mmol) of ammonium acetate, 50 mL of glacial acetic acid, and 13.2 mmol of the corresponding substituted benzaldehyde. The mixture was kept under reflux and magnetic stirring for 4 h, using an oil bath for heating, and afterward, 100 mL of ice-cold deionized water was added to induce precipitation. The precipitate was filtered out under vacuum, washed with deionized water (5 × 15 mL), and dried under suction. The crude product was dissolved in 300 mL of EtOAc, dried under $MgSO_4$, filtered, concentrated through rotary evaporation, and dried under vacuum (10^{-3} mbar, 30 min). Purification was attained using recrystallization from hot EtOAc or CH_2Cl_2/hexane. The obtained cotton wool-like crystals were slightly yellow, being filtered under vacuum, washed with cold pentane (2 × 50 mL), and dried under vacuum (10^{-3} mbar, 30 min).

*2,4,5-Triphenylimidazole (**L1**).* 1.98 g (52%), slightly yellow cotton wool-like crystals, R_f = 0.53 (SiO_2, Hex/EtOAc 3:1). Anal. Calcd for $C_{21}H_{16}N_2$: C, 85.1; H, 5.4; N, 9.4. Found: C, 84.5; H, 5.4; N, 9.3. ^{1}H NMR (DMSO-d_6, 300 MHz): δ 12.71 (s, 1H), 8.13−8.09 (m, 2H), 7.55−7.23 (m, 13H). ^{13}C{^{1}H} NMR (DMSO-d_6, 75 MHz): δ 145.6, 137.1, 135.2, 131.1, 130.4, 128.7, 128.5, 128.3, 127.8, 127.1, 126.5, 125.2.

*2-(4-Methoxyphenyl)-4,5-diphenylimidazole (**L2**).* 2.77 g (66%), slightly yellow cotton wool-like crystals, R_f = 0.67 (SiO_2, Hex/EtOAc 3:1). Anal. Calcd for $C_{22}H_{18}N_2O$: C, 80.9; H, 5.6; N, 8.6. Found: C, 80.9; H, 5.5; N, 8.5. ^{1}H NMR (DMSO-d_6, 300 MHz): δ 12.52 (s, 1H), 8.03 (d, 2H, J = 8.8 Hz), 7.56−7.22 (m, 10H), 7.05 (d, 2H, J = 8.9 Hz), 3.82 (s, 3H). ^{13}C{^{1}H} NMR (DMSO-d_6, 75 MHz): δ 159.4, 145.6, 136.8, 135.3, 131.2, 128.6, 128.4, 128.2, 127.6, 127.1, 126.7, 126.4, 123.1, 114.1, 55.2.

*4,5-Diphenyl-2-(p-tolyl)imidazole (**L3**).* 1.35 g (34%), slightly yellow cotton wool-like crystals, R_f = 0.58 (SiO_2, Hex/EtOAc 3:1). Anal. Calcd for $C_{22}H_{18}N_2$: C, 85.1; H, 5.8; N, 9.0. Found: C, 83.6; H, 5.6; N, 9.5. ^{1}H NMR ($CDCl_3$, 500 MHz): δ 7.79 (d, 2H, J = 8.2 Hz), 7.53 (d, 4H, J = 7.1 Hz), 7.34−7.26 (m, 6H), 7.23 (d, 2H, J = 7.9 Hz), 2.38 (s, 3H). ^{13}C{^{1}H} NMR ($CDCl_3$, 125 MHz): δ 146.4, 138.9, 129.7, 128.7, 128.0, 127.5, 127.2, 125.4, 21.5.

*2-(4-Bromophenyl)-4,5-diphenylimidazole (**L4**).* 4.5 g (93%), slightly yellow cotton wool-like crystals, R_f = 0.53 (SiO_2, Hex/EtOAc 3:1). Anal. Calcd for $C_{21}H_{15}N_2Br$: C, 67.2; H, 4.0; Br, 21.3; N,

https://doi.org/10.1021/acs.joc.1c00230
J. Org. Chem. 2021, 86, 6633−6647

7.5. Found: C, 67.9; H, 4.1; Br, 21.4; N, 7.4. ^{1}H NMR (DMSO-d_6, 300 MHz): δ 12.80 (s, 1H), 8.07−8.02 (m, 2H), 7.71−7.67 (m, 2H), 7.53 (d, 4H, J = 6.9 Hz), 7.37 (s, 6H). ^{13}C{^{1}H} NMR (DMSO-d_6, 75 MHz): δ 144.5, 131.7, 129.5, 128.5, 127.1, 121.4.

*4,5-Diphenyl-2-(4-(trifluoromethyl)phenyl)imidazole (**L5**).* 2.1 g (45%), slightly yellow cotton wool-like crystals, R_f = 0.65 (SiO_2, Hex/EtOAc 3:1). Anal. Calcd for $C_{22}H_{15}F_3N_2$: C, 72.5; H, 4.1; N, 7.7. Found: C, 71.8; H, 3.8; N, 8.1. ^{1}H NMR ($CDCl_3$, 500 MHz): δ 8.03 (d, 2H, J = 8.1 Hz), 7.70 (ddd, 2H, J = 8.1, 4.4, 2.0 Hz), 7.57−7.52 (m, 4H), 7.34 (dt, 6H, J = 13.6, 7.7 Hz). ^{13}C{^{1}H} NMR ($CDCl_3$, 125 MHz): δ 168.0, 144.5, 133.1, 131.0, 128.8, 128.0, 126.0, 126.0, 125.4.

*4-(4,5-Diphenylimidazol-2-yl)benzonitrile (**L6**).* 2.60 g (62%), slightly yellow cotton wool-like crystals, R_f = 0.23 (SiO_2, Hex/EtOAc 4:1). Anal. Calcd for $C_{22}H_{15}N_3$: C, 82.2; H, 4.7; N, 13.1. Found: C, 81.2; H, 5.5; N, 11.2. ^{1}H NMR (DMSO-d_6, 500 MHz): δ 13.00 (1 H, s), 8.25 (d, 2H, J = 8.4 Hz), 7.93 (d, 2H, J = 8.4 Hz), 7.58−7.20 (m, 10H). ^{13}C{^{1}H} NMR (DMSO-d_6, 125 MHz): δ 143.7, 138.1, 134.7, 134.3, 132.8, 130.6, 129.6, 128.7, 128.5, 128.3, 128.2, 127.1, 126.8, 125.5, 118.9, 110.1.

Hydroperoxide H1−6 Preparation. Based on the method of Lu et al.,[3] a 100 mL Schlenk reaction tube was charged with 80 mL of a 5:1 CH_2Cl_2/ACN mixture and 0.61 mmol of **L1-6**. A catalytic amount of methylene blue was added, the mixture was kept under magnetic stirring, and molecular oxygen was bubbled using a glass tube with a fritted glass tip. The solution was irradiated under a 665 nm light-emitting diode array, while the temperature was maintained at 4 °C using a water−ice bath. The singlet oxygen produced through photosensitization reacted with the imidazolyl moiety of **L1-6** by an *ene* reaction, producing hydroperoxides **H1−6**. The reaction was followed using thin-layer chromatography, and the organic peroxide was revealed with a potassium iodide solution in acetic acid. After completion, the reaction mixture was filtered through a 2.5 × 10 cm silica gel layer and eluted with CH_2Cl_2. Hydroperoxides were purified through recrystallization from CH_2Cl_2/pentane, filtered under vacuum using a fritted glass Büchner funnel, and washed with cold pentane (2 × 50 mL). The obtained colorless cotton-like crystals were dried under vacuum for 3 h (10^{-3} mbar). We were unable to purify **H6** adequately for characterization, even after many recrystallization cycles; nonetheless, **H6** was still used for the preparation of **S6**.

*4-Hydroperoxy-2,4,5-Triphenyl-4-Imidazole (**H1**).* 0.140 g (63%), colorless crystals, R_f = 0.41 (SiO_2, Hex/EtOAc 3:1). Anal. Calcd for $C_{21}H_{16}N_2O_2$: C, 76.8; H, 4.9; N, 8.5. Found: C, 73.1; H, 4.8; N, 7.6. ^{1}H NMR ($CDCl_3$, 500 MHz): δ 8,41−8.39 (m, 2H), 7.92−7.91 (m, 2H), 7.60 (ddd, 1H, J = 6.7, 3.8, 1.1 Hz), 7.55−7.50 (m, 4H), 7.35−7.32 (m, 4H), 7.2 (t, 2H, J = 7.8 Hz), 1.66 (s, 1H). ^{13}C{^{1}H} NMR ($CDCl_3$, 125 MHz): δ 191.4, 172.5, 134.7, 133.3, 132.3, 130.8, 130.3, 130.0, 129.9, 129.6, 128.9, 128.9, 128.5, 126.8, 115.5.

*4-Hydroperoxy-2-(4-methoxyphenyl)-4,5-diphenyl-4-imidazole (**H2**).* 0.157 g (71%), colorless crystals, R_f = 0.23 (SiO_2, Hex/EtOAc 3:1). Anal. Calcd for $C_{22}H_{18}N_2O_3$: C, 73.7; H, 5.1; N, 7.8. Found: C, 73.5; H, 5.1; N, 7.6. ^{1}H NMR ($CDCl_3$, 500 MHz): δ 8.40−8.38 (m, 2H), 7.92−7.89 (m, 2H), 7.60−7.57 (m, 1H), 7.53−7.50 (m, 4H), 7.34−7.31 (m, 3H), 6.70−6.67 (m, 2H), 3.82 (s, 3H), 1.69 (m, 1H). ^{13}C{^{1}H} NMR ($CDCl_3$, 125 MHz): δ 190.8, 171.9, 162.9, 135.1, 133.1, 132.1, 130.9, 130.3, 129.4, 128.9, 128.8, 126.7, 122.8, 115.3, 113.8, 55.5.

*4-Hydroperoxy-4,5-Diphenyl-2-(p-Tolyl)-4-Imidazole (**H3**).* 0.168 g (76%), colorless crystals, R_f = 0.38 (SiO_2, Hex/EtOAc 3:1). Anal. Calcd for $C_{22}H_{18}N_2O_2$: C, 77.2; H, 5.3; N, 8.2. Found: C, 72.6; H, 4.9; N, 8.4. ^{1}H NMR ($CDCl_3$, 500 MHz): δ 8.40 (d, 2H, J = 7.3 Hz), 7.81 (d, 2H, J = 8.0 Hz), 7.59 (t, 1H, J = 7.3 Hz), 7.53−7.51 (m, 4H), 7.33−7.32 (m, 3H), 6.98 (d, 2H, J = 8.0 Hz), 2.32 (s, 3H), 1.66 (s, 1H). ^{13}C{^{1}H} NMR ($CDCl_3$, 125 MHz): δ 191.1, 172.4, 142.9, 134.9, 133.2, 130.9, 130.3, 130.0, 129.5, 129.0, 128.9, 128.9, 127.3, 126.8, 115.3, 21.8.

*2-(4-Bromophenyl)-4-hydroperoxy-4,5-diphenyl-4-imidazole (**H4**).* 0.190 g (77%), colorless crystals, R_f = 0.48 (SiO_2, Hex/EtOAc 3:1). Anal. Calcd for $C_{21}H_{15}BrN_2O_2$: C, 61.9; H, 3.7; N, 6.9. Found: C, 61.8; H, 3.9; N, 6.6. ^{1}H NMR ($CDCl_3$, 500 MHz): δ 8.38 (dt, 2H, J = 8.5, 1.6 Hz), 7.76−7.73 (m, 2H), 7.64−7.60 (m, 1H), 7.55−7.52 (m, 2H), 7.49−7.47 (m, 2H), 7.38−7.32 (m, 5H), 1.62 (s, 1H). ^{13}C{^{1}H} NMR ($CDCl_3$, 125 MHz): δ 191.7, 171.7, 134.4, 133.6, 131.8, 131.3, 130.6, 130.4, 129.8, 129.0, 129.0, 128.8, 127.8, 126.8, 115.7.

*4-Hydroperoxy-4,5-diphenyl-2-(4-(trifluoromethyl)phenyl)-4-imidazole (**H5**).* 0.184 g (85%), colorless crystals, R_f = 0.78 (SiO_2, Hex/EtOAc 3:1). Anal. Calcd for $C_{22}H_{15}F_3N_2O_2$: C, 66.7; H, 3.8; N, 7.1. Found: C, 69.5; H, 4.8; N, 6.9. ^{1}H NMR ($CDCl_3$, 500 MHz): δ 8.41−8.39 (m, 2H), 7.97 (d, 2H, J = 8.1 Hz), 7.66−7.63 (m, 1H), 7.57−7.53 (m, 2H), 7.50−7.48 (m, 2H), 7.44 (d, 2H, J = 8.2 Hz), 7.37−7.33 (m, 3H), 1.59 (s, 1H). ^{13}C{^{1}H} NMR ($CDCl_3$, 125 MHz): δ 192.2, 171.3, 134.1, 133.9, 133.2, 130.5, 130.1, 129.9, 129.4, 129.1, 128.5, 126.8, 125.5, 125.5, 115.9.

Silylperoxide S1−6 Preparation. Based on the method of Lu et al.,[3] a 25 mL round-bottom flask was charged with 10 mL of CH_2Cl_2, **H1-6** (0.92 mmol), imidazole (4.6 mmol), and TBDMSCl (3.7 mmol). The mixture was kept under vigorous magnetic stirring at room temperature for 1 h. The reaction was followed using thin-layer chromatography (20:1 hexane/EtOAc), and the presence of **S1−6** was tested using a TBAF solution in THF (1.0 mol L^{-1}), which caused a rapid light flash on the thin-layer chromatography spot containing the peroxide. After that, the solution was filtered and the CH_2Cl_2 removed by rotary evaporation. The obtained solid was solubilized with hexane and washed with an equal volume of deionized water (5×) to remove the residual salt. To the organic layer, $MgSO_4$ was added, the mixture was filtered, and the solvent removed by rotary evaporation and dried under vacuum (10^{-3} mbar, 30 min). Silylperoxides **S1−6** were purified by flash column chromatography (SiO_2, hexane/EtOAc 9:1), and after solvent removal, the clear colorless crystals were dried under vacuum (10^{-3} mbar, 90 min).

*4-((tert-Butyldimethylsilyl)peroxy)-2,4,5-triphenyl-4-imidazole (**S1**).* 0.190 g (26%), colorless crystals, R_f = 0.61 (SiO_2, Hex/EtOAc 9:1). Anal. Calcd for $C_{27}H_{30}N_2O_2Si$: C, 73.3; H, 6.8; N, 6.3. Found: C, 74.3; H, 6.9; N, 6.6. ^{1}H NMR ($CDCl_3$, 500 MHz): δ 8.50−8.48 (m, 2H), 8.24 (ddd, 2H, J = 7.3, 3.0, 1.6 Hz), 7.59−7.50 (m, 4H), 7.46−7.43 (m, 2H), 7.35−7.31 (m, 2H), 7.30−7.27 (m, 3H), 0.85 (s, 9H), 0.21 (s, 3H), 0.16 (s, 3H). ^{13}C{^{1}H} NMR ($CDCl_3$, 125 MHz): δ 191.3, 171.6, 134.8, 132.5, 132.0, 131.6, 131.1, 130.0, 129.8, 129.2, 128.8, 128.7, 128.6, 126.2, 115.2, 26.2, 18.5, −5.3, −5.4.

*4-((tert-Butyldimethylsilyl)peroxy)-2-(4-methoxyphenyl)-4,5-diphenyl-4-imidazole (**S2**).* 0.113 g (26%), colorless crystals, R_f = 0.36 (SiO_2, Hex/EtOAc 9:1). Anal. Calcd for $C_{28}H_{32}N_2O_3Si$: C, 71.1; H, 6.8; N, 5.9. Found: C, 71.9; H, 6.8; N, 6.0. ^{1}H NMR ($CDCl_3$, 500 MHz): δ 8.46 (d, 2H, J = 4.4 Hz), 8.23−8.21 (m, 2H), 7.53−7.50 (m, 1H), 7.45−7.42 (m, 2H), 7.33−7.27 (m, 5H), 7.03 (d, 2H, J = 8.5 Hz), 3.90 (s, 3H), 0.85 (s, 9H), 0.21 (s, 3H), 0.16 (s, 3H). ^{13}C{^{1}H} NMR ($CDCl_3$, 125 MHz): δ 192.3, 190.8, 171.2, 135.1, 132.5, 132.0, 131.1, 129.8, 129.1, 128.8, 128.6, 126.1, 114.1, 55.6, 26.2, 18.4, −5.3, −5.3.

*4-((tert-Butyldimethylsilyl)peroxy)-4,5-diphenyl-2-(p-tolyl)-4-imidazole (**S3**).* 0.128 g (30%), colorless crystals, R_f = 0.57 (SiO_2, Hex/EtOAc 9:1). Anal. Calcd for $C_{28}H_{32}N_2O_2Si$: C, 73.6; H, 7.1; N, 6.1. Found: C, 73.9; H, 7.1; N, 6.1. ^{1}H NMR ($CDCl_3$, 500 MHz): δ 8.39 (d, 2H, J = 7.7 Hz), 8.23 (d, 2H, J = 7.4 Hz), 7.51 (t, 1H, J = 7.1 Hz), 7.44 (t, 2H, J = 7.4 Hz), 7.31 (dd, 7H, J = 26.8, 4.9 Hz), 2.46 (s, 3H), 0.86 (s, 9H), 0.21 (s, 3H), 0.16 (s, 3H). ^{13}C{^{1}H} NMR ($CDCl_3$, 125 MHz): δ 191.1, 171.6, 134.9, 132.5, 131.1, 130.1, 129.8, 129.4, 129.1, 128.8, 128.5, 126.1, 115.1, 26.2, 21.9, 18.4, −5.3, −5.3.

*2-(4-Bromophenyl)-4-((tert-butyldimethylsilyl)peroxy)-4,5-diphenyl-4-imidazole (**S4**).* 0.090 g (22%), colorless crystals, R_f = 0.59 (SiO_2, Hex/EtOAc 9:1). Anal. Calcd for $C_{27}H_{29}BrN_2O_2Si$: C, 62.2; H, 5.6; N, 5.4. Found: C, 63.0; H, 5.7; N, 5.5. ^{1}H NMR ($CDCl_3$, 500 MHz): δ 8.40−8.37 (m, 2H), 8.27−8.25 (m, 2H), 7.69−7.67 (m, 2H), 7.55−7.51 (m, 1H), 7.48−7.44 (m, 2H), 7.38−7.34 (m, 2H), 7.32−7.29 (m, 3H), 0.88 (s, 9H), 0.23 (s, 3H), 0.19 (s, 3H). ^{13}C{^{1}H} NMR ($CDCl_3$, 125 MHz): δ 191.6, 170.7, 134.6, 132.7, 131.9, 131.4, 130.9, 130.5, 129.9, 129.3, 128.8, 128.6, 126.9, 126.2, 115.3, 26.2, 18.4, −5.3, −5.4.

https://doi.org/10.1021/acs.joc.1c00230
J. Org. Chem. 2021, 86, 6633−6647

*4-((tert-Butyldimethylsilyl)peroxy)-4,5-diphenyl-2-(4-(trifluoromethyl)phenyl)-4-imidazole (**S5**).* 0.046 g (40%), colorless crystals, R_f = 0.61 (SiO_2, Hex/EtOAc 9:1). Anal. Calcd for $C_{28}H_{29}F_3N_2O_2Si$: C, 65.9; H, 5.7; N, 5.5. Found: C, 66.2; H, 5.9; N, 5.5. ^{1}H NMR ($CDCl_3$, 500 MHz): δ 8.60 (d, 2H, J = 8.0 Hz), 8.25−8.23 (m, 2H), 7.78 (d, 2H, J = 8.1 Hz), 7.57−7.53 (m, 1H), 7.48−7.45 (m, 2H), 7.35−7.29 (m, 5H), 0.85 (s, 9H), 0.20 (s, 3H), 0.16 (s, 3H). ^{13}C{^{1}H} NMR ($CDCl_3$, 125 MHz): δ 192.0, 170.4, 134.8, 134.3, 133.6, 133.4, 133.0, 130.9, 130.3, 130.0, 129.5, 128.9, 128.7, 126.3, 125.6, 125.6, 125.1, 115.3, 26.2, 18.4, −5.4, −5.4.

*4-(4-((tert-Butyldimethylsilyl)peroxy)-4,5-diphenyl-4-imidazole-2-benzonitrile (**S6**).* 0.110 g (61%), colorless crystals, R_f = 0.72 (SiO_2, Hex/EtOAc 9:1). Anal. Calcd for $C_{28}H_{29}N_3O_2Si$: C, 71.9; H, 6.2; N, 9.0. Found: C, 71.6; H, 6.2; N, 8.9. ^{1}H NMR ($CDCl_3$, 500 MHz): δ 8.58−8.56 (m, 2H), 8.24−8.22 (m, 2H), 7.82−7.80 (m, 2H), 7.57−7.54 (m, 1H), 7.48−7.45 (m, 2H), 7.33−7.29 (m, 5H), 0.84 (s, 9H), 0.19 (s, 3H), 0.16 (s, 3H). ^{13}C{^{1}H} NMR ($CDCl_3$, 125 MHz): δ 192.3, 170.0, 135.7, 134.3, 133.0, 132.4, 130.9, 130.3, 130.0, 129.6, 128.9, 128.7, 126.4, 118.6, 115.5, 115.2, 26.1, 18.4, −5.4, −5.4.

Quantum Yield Determination. Fluorescence quantum yields (Φ_{FL}) were determined using the relative method[32] with 2,5-diphenyloxazole in EtOAc as the standard. Chemiluminescence quantum yields (Φ_{CL}) were obtained from the integrated CL intensity−time profiles, using the method reported elsewhere.[4,25] Singlet excited-state formation quantum yields (Φ_S) were determined by numerically dividing Φ_{CL} by Φ_{FL}, as described elsewhere.[4,25]

Chemiluminescence Kinetic Measurements for S1−6 Using the Luminometer. The 1.5 μmol L^{-1} stock solutions of **S1−6** were prepared in ACN, and the 1.5 mmol L^{-1} TBAF stock solution in THF was obtained by diluting 15 μL of a commercial 1.0 mol L^{-1} TBAF solution in THF up to 10 mL of the solvent. The luminometer test tube was charged with 1.7 mL of the silylperoxide stock solution and placed in the equipment measurement chamber. After 4 s of initiating data acquisition, the two automatic injectors of the luminometer were used to add, simultaneously, the TBAF stock solution and pure THF solvent. By changing the setup volumes of the two injectors accordingly, it was possible to have different final concentrations of TBAF, diluting the stock solution directly into the test tube containing **S1−6**. Combined, the added volume from the two injectors was always 300 μL so as to keep the final volume in the test tube at 2.0 mL and the final concentration of silylperoxide at 1.27 μmol L^{-1}. The used TBAF concentrations are reported in Tables S1−S6.

Chemiluminescence Kinetic Measurements for S1, S2, and S4 Using the Fluorescence Spectrophotometer. Using stock solutions of 0.025 mmol L^{-1} for **S1**, **S2**, and **S4** and 25.0 mmol L^{-1} for TBAF, CL kinetic assays were performed by varying the TBAF concentration from 0.25 to 2.0 mmol L^{-1}, keeping peroxide concentrations constant. Data acquisition was initiated after quick addition of the TBAF stock solution to induce the peroxide decomposition. The voltage of the photomultiplier was 1000 V, and the opening of the emission slit was 20 nm for the kinetic experiments with all studied silylperoxides.

Chemiluminescence Kinetic Measurements for H1−5 Using the Fluorescence Spectrophotometer. Using stock solutions 0.2 mmol L^{-1} for **H1−5** and 0.2 mol L^{-1} for DBU, CL kinetic assays were performed by varying the DBU concentration from 1.0 to 10.0 mmol L^{-1}, keeping peroxide concentrations constant. Data acquisition was initiated after quick addition of the DBU stock solution to induce the peroxide decomposition. The voltage of the photomultiplier was 800 V, and the opening of the emission slit was 10 nm for the kinetic experiments with all studied hydroperoxides.

■ ASSOCIATED CONTENT

Supporting Information

The Supporting Information is available free of charge at https://pubs.acs.org/doi/10.1021/acs.joc.1c00230.

Kinetic CL data for the induced decomposition of silylperoxides (**S1−6**) and hydroperoxides (**H1−5**), absorbance, fluorescence, and NMR spectral data, and examples of CL time profiles and linear correlations with observed rate constants (PDF)

■ AUTHOR INFORMATION

Corresponding Author

Fernando Heering Bartoloni − *Centro de Ciências Naturais e Humanas, Universidade Federal do ABC, Santo André 09210-580, São Paulo, Brazil;* orcid.org/0000-0001-7304-0992; Email: fernando.bartoloni@ufabc.edu.br

Authors

Andreia Boaro − *Centro de Ciências Naturais e Humanas, Universidade Federal do ABC, Santo André 09210-580, São Paulo, Brazil*

Roberta Albino Reis − *Centro de Ciências Naturais e Humanas, Universidade Federal do ABC, Santo André 09210-580, São Paulo, Brazil*

Carolina Santana Silva − *Centro de Ciências Naturais e Humanas, Universidade Federal do ABC, Santo André 09210-580, São Paulo, Brazil*

Diêgo Ulysses Melo − *Centro de Ciências Naturais e Humanas, Universidade Federal do ABC, Santo André 09210-580, São Paulo, Brazil*

Alexander Garreta Gonçalves Costa Pinto − *Centro de Ciências Naturais e Humanas, Universidade Federal do ABC, Santo André 09210-580, São Paulo, Brazil*

Complete contact information is available at: https://pubs.acs.org/10.1021/acs.joc.1c00230

Notes

The authors declare no competing financial interest.

■ ACKNOWLEDGMENTS

This study was financed in part by the Coordenação de Aperfeiçoamento de Pessoal de Nível Superior—Brasil (CAPES)—Finance Code 001; D.U.M. and R.A.R. are thankful to CAPES for the fellowships. The authors are thankful to the Fundação de Amparo à Pesquisa do Estado de São Paulo (FAPESP) for the provided grants (A.B. 2016/10585-4 and 2019/15871-3, F.H.B. 2012/13807-7). The authors are grateful to the Multiuser Central Facilities at UFABC for the experimental support.

■ REFERENCES

(1) Radziszewski, B. R. Untersuchungen Über Hydrobenzamid, Amarin Und Lophin. *Ber. Dtsch. Chem. Ges.* **1877**, *10*, 70−75.

(2) Wiedemann, E.; Messerschmitt, J. B. Ueber Fluorescenz Und Phosphorescenz II. Abhandlung. Gültigkeit Des Talbot' Schen Gesetzes. *Ann. Phys.* **1888**, *270*, 446−463.

(3) Lu, G.; Wada, J.; Kimoto, T.; Iga, H.; Nishigawa, H.; Kimura, M.; Hu, Z. Chemiexcitation of the Chemiluminescence of Lophine Peroxide Anions via a Partially Cyclic Transition State. *Eur. J. Org Chem.* **2014**, *2014*, 1212−1219.

(4) Vacher, M.; Galván, I. F.; Ding, B.-W.; Schramm, S.; Berraud-Pache, R.; Naumov, P.; Ferré, N.; Liu, Y.-J.; Navizet, I.; Roca-Sanjuán, D.; Baader, W. J.; Lindh, R. Chemi- and Bioluminescence of Cyclic Peroxides. *Chem. Rev.* **2018**, *118*, 6927−6974.

(5) Bastos, E. L.; Farahani, P.; Bechara, E. J. H.; Baader, W. J. Four-membered cyclic peroxides: Carriers of chemical energy. *J. Phys. Org. Chem.* **2017**, *30*, No. e3725.

(6) Augusto, F. A.; Francés-Monerris, A.; Galván, I. F.; Roca-Sanjuán, D.; Bastos, E. L.; Baader, W. J.; Lindh, R. Mechanism of

activated chemiluminescence of cyclic peroxides: 1,2-dioxetanes and 1,2-dioxetanones. *Phys. Chem. Chem. Phys.* **2017**, *19*, 3955−3962.
(7) Augusto, F. A.; de Souza, G. A.; Khalid, M.; Baader, W. J. Efficiency of electron transfer initiated chemiluminescence. *Photochem. Photobiol.* **2013**, *89*, 1299−1317.
(8) Bastos, E. L.; da Silva, S. M.; Baader, W. J. Solvent cage effects: Basis of a general mechanism for efficient chemiluminescence. *J. Org. Chem.* **2013**, *78*, 4432−4439.
(9) Ciscato, L. F. M. L.; Augusto, F. A.; Weiss, D.; Bartoloni, F. H.; Albrecht, S.; Brandl, H.; Zimmermann, T.; Baader, W. J. The chemiluminescent peroxyoxalate system: state of the art almost 50 years from its discovery. *Arkivoc* **2012**, *2012*, 391−430.
(10) Roda, A. *Chemiluminescence and Bioluminescence: Past, Present and Future*; Roda, A., Ed.; Royal Society of Chemistry, 2010.
(11) Baader, W. J.; Stevani, C. V.; Bastos, E. L. *The Chemistry of Peroxides, Parts 1 & 2*; Waldvogel, S., Ed.; John Wiley & Sons, Inc., 2006.
(12) Davidson, D.; Weiss, M.; Jelling, M. The Action of Ammonia on Benzil. *J. Org. Chem.* **1937**, *02*, 319−327.
(13) White, E. H.; Harding, M. J. C. Chemiluminescence in Liquid Solutions: The Chemiluminescence of Lophine and Its Derivatives. *Photochem. Photobiol.* **1965**, *4*, 1129−1155.
(14) White, E. H.; Harding, M. J. C. The Chemiluminescence of Lophine and Its Derivatives. *J. Am. Chem. Soc.* **1964**, *86*, 5686−5687.
(15) Sonnenberg, J.; White, D. M. Chemiluminescent and Thermochemiluminescent Lophine Hydroperoxide. *J. Am. Chem. Soc.* **1964**, *86*, 5685−5686.
(16) White, E. H.; Rapaport, E.; Seliger, H. H.; Hopkins, T. A. The chemi- and bioluminescence of firefly luciferin: An efficient chemical production of electronically excited states. *Bioorg. Chem.* **1971**, *1*, 92−122.
(17) da Silva, L. P.; da Silva, J. C. G. E. Theoretical study of the correlation between superoxide anion consumption and firefly luciferin chemiluminescence. *Chem. Phys. Lett.* **2013**, *577*, 127−130.
(18) Branchini, B. R.; Behney, C. E.; Southworth, T. L.; Fontaine, D. M.; Gulick, A. M.; Vinyard, D. J.; Brudvig, G. W. Experimental support for a single electron-transfer oxidation mechanism in firefly bio- luminescence. *J. Am. Chem. Soc.* **2015**, *137*, 7592−7595.
(19) Kondo, H.; Igarashi, T.; Maki, S.; Niwa, H.; Ikeda, H.; Hirano, T. Substituent Effects on the Kinetics for the Chemiluminescence Reaction of 6-Arylimidazo[1,2-a]Pyrazin-3(7H)-Ones (Cypridina Luciferin Analogues): Support for the Single Electron Transfer (SET)-Oxygenation Mechanism with Triplet Molecular Oxygen. *Tetrahedron Lett.* **2005**, *46*, 7701−7704.
(20) Philbrook, G. E.; Maxwell, M. A. Chemiluminescent Intensities from Substituted Lophines. *Tetrahedron Lett.* **1964**, *5*, 1111−1116.
(21) Kimura, M.; Nishikawa, H.; Kura, H.; Lim, H.; White, E. H. Maximization of the Chemiluminescence Efficiency of 1,4,5-Triarylhydroperoxy-4H-Isoimidazoles. *Chem. Lett.* **1993**, *22*, 505−508.
(22) Benisvy, L.; Blake, A. J.; Collison, D.; Davies, E. S.; David Garner, C.; McInnes, E. J. L.; McMaster, J.; Whittaker, G.; Wilson, C. A Phenol-Imidazole pro-Ligand That Can Exist as a Phenoxyl Radical, Alone and When Complexed to Copper(II) and Zinc(II). *Dalton Trans.* **2003**, *10*, 1975−1985.
(23) Reis, R. A.; Boaro, A.; Orfão, R. B.; Melo, D. U.; Bartoloni, F. H. The Decomposition of Triphenylimidazole-Para-Acetate Follows Specific Base Catalysis and Can Be Conveniently Followed by Fluorescence. *Luminescence* **2019**, *34*, 234−242.
(24) Orfão, R. B.; De Carvalho, F.; Homem-De-Mello, P.; Bartoloni, F. H. On the Fluorescent, Steric and Electronic Factors Affecting the Detection of Metallic Ions Using an Imidazolyl-Phenolic Derived Fluorescent Probe. *J. Braz. Chem. Soc.* **2017**, *28*, 1896−1904.
(25) Alves, J.; Boaro, A.; da Silva, J. S.; Keslarek, V. B.; Cabral, C. A.; Orfão, R. B.; Ciscato, L. F. M. L., Jr.; Bartoloni, F. H. Lophine Derivatives as Activators in Peroxyoxalate Chemiluminescence. *Photochem. Photobiol. Sci.* **2015**, *14*, 320−328.
(26) Ciscato, L. F. M. L.; Bartoloni, F. H.; Weiss, D.; Beckert, R.; Baader, W. J. Experimental Evidence of the Occurrence of Intramolecular Electron Transfer in Catalyzed 1,2-Dioxetane Decomposition. *J. Org. Chem.* **2010**, *75*, 6574−6580.
(27) Nery, A. L. P.; Weiß, D.; Catalani, L. H.; Baader, W. J. Studies on the Intramolecular Electron Transfer Catalyzed Thermolysis of 1,2-Dioxetanes. *Tetrahedron* **2000**, *56*, 5317−5327.
(28) Nakashima, K. Lophine Derivatives as Versatile Analytical Tools. *Biomed. Chromatogr.* **2003**, *17*, 83−95.
(29) Anslyn, E.V.; Dougherty, D. A. *Modern Physical Organic Chemistry*; University Science Books, 2006.
(30) Adam, W. Determination of Chemiexcitation Yields in the Thermal Generation of Electronic Excitation from 1,2-Dioxetanes. In *Chemical and Biological Generation of Excited States*; Adam, W., Ed.; Elsevier, Inc., 2012.
(31) Wilson, T. Chemiluminescence in the Liquid Phase: Thermal Cleavage of Dioxetanes. *Int. Rev. Sci.: Phys. Chem., Ser. Two* **1976**, *9*, 265−311.
(32) Stevani, C. V.; Silva, S. M.; Baader, W. J. Studies on the Mechanism of the Excitation Step in Peroxyoxalate Chemiluminescence. *Eur. J. Org Chem.* **2000**, *2000*, 4037−4046.
(33) De Carvalho, F.; Neto, M. D. C.; Bartoloni, F. H.; Homem-de-Mello, P. Density Functional Theory Applied to Excited State Intramolecular Proton Transfer in Imidazole-, Oxazole-, and Thiazole-Based Systems. *Molecules* **2018**, *23*, 1231.
(34) Sedgwick, A. C.; Wu, L.; Han, H.-H.; Bull, S. D.; He, X.-P.; James, T. D.; Sessler, J. L.; Tang, B. Z.; Tian, H.; Yoon, J. Excited-State Intramolecular Proton-Transfer (ESIPT) Based Fluorescence Sensors and Imaging Agents. *Chem. Soc. Rev.* **2018**, *47*, 8842−8880.
(35) Duarte, L. G. T. A.; Germino, J. C.; Berbigier, J. F.; Barboza, C. A.; Faleiros, M. M.; De Alencar Simoni, D.; Galante, M. T.; De Holanda, M. S.; Rodembusch, F. S.; Atvars, T. D. Z. White-Light Generation from All-Solution-Processed OLEDs Using a Benzothiazole-Salophen Derivative Reactive to the ESIPT Process. *Phys. Chem. Chem. Phys.* **2019**, *21*, 1172−1182.
(36) Chen, C.-L.; Chen, Y.-T.; Demchenko, A. P.; Chou, P.-T. Amino Proton Donors in Excited-State Intramolecular Proton-Transfer Reactions. *Nat. Rev. Chem.* **2018**, *2*, 131−143.
(37) El Seoud, O. A.; Baader, W. J.; Bastos, E. L. Practical Chemical Kinetics in Solution. *In Encyclopedia of Physical Organic Chemistry*; John Wiley & Sons, Inc., 2016.
(38) Augusto, F. A.; Bartoloni, F. H.; Cabello, M. C.; dos Santos, A. P. F.; Baader, W. J. Kinetic Studies on 2,6-Lutidine Catalyzed Peroxyoxalate Chemiluminescence in Organic and Aqueous Medium: Evidence for General Base Catalysis. *J. Photochem. Photobiol. Chem.* **2019**, *382*, 111967.
(39) Cabello, M. C.; El Seoud, O. A. A.; Baader, W. J. Effect of Ionic Liquids on the Kinetics and Quantum Efficiency of Peroxyoxalate Chemiluminescence in Aqueous Media. *J. Photochem. Photobiol. Chem.* **2018**, *367*, 471−478.
(40) Souza, G. A.; Lang, A. P.; Baader, W. J. Mechanistic Studies on the Peroxyoxalate Chemiluminescence Using Sodium Salicylate as Base Catalyst. *Photochem. Photobiol.* **2017**, *93*, 362−369.
(41) Silva, S. M.; Casallanovo, F. l.; Oyamaguchi, K. H.; Ciscato, L. F. L. M.; Stevani, C. V.; Baader, W. J. Kinetic Studies on the Peroxyoxalate Chemiluminescence Reaction: Determination of the Cyclization Rate Constant. *Luminescence* **2002**, *17*, 313−320.
(42) Stevani, C. V.; Lima, D. c. F.; Toscano, V. G.; Baader, W. J. Kinetic Studies on the Peroxyoxalate Chemiluminescent Reaction: Imidazole as a Nucleophilic Catalyst. *J. Chem. Soc., Perkin Trans. 2* **1996**, *2*, 989−995.
(43) Quina, F. H.; Bastos, E. L.. Fundamental Aspects of Quantitative Structure-Reactivity Relationships. In *Encyclopedia of Physical Organic Chemistry*; Wang, Z., Ed.; John Wiley & Sons, Inc., 2017.
(44) The use of Hammett plots for the determination of organic reactions mechanisms is, beyond doubt, extremely valuable (see refs 29 and 43, for example). It should be noted that this linear free-energy relationship also made significant contributions to the study of chemiluminescence and its reaction pathways. Examples of Hammett

https://doi.org/10.1021/acs.joc.1c00230
J. Org. Chem. 2021, 86, 6633−6647

plots being used in chemiluminescence, under very different contexts, can be found in refs 25 and 26.
(45) Linnell, R. Dissociation Constants of 2-Substituted Pyridines. *J. Org. Chem.* **1960**, *25*, 290.
(46) Walba, H.; Isensee, R. W. Acidity Constants of Some Arylimidazoles and Their Cations. *J. Org. Chem.* **1961**, *26*, 2789−2791.
(47) Hall, H. K. Correlation of the Base Strengths of Amines. *J. Am. Chem. Soc.* **1957**, *79*, 5441−5444.
(48) Kaupmees, K.; Trummal, A.; Leito, I. Basicities of Strong Bases in Water: A Computational Study. *Croat. Chem. Acta* **2014**, *87*, 385−395.
(49) Jonsson, M. Thermochemical Properties of Peroxides and Peroxyl Radicals. *J. Phys. Chem.* **1996**, *100*, 6814−6818.
(50) Boaro, A.; Bartoloni, F. H. Peroxyoxalate High-Energy Intermediate Is Efficiently Decomposed by the Catalyst Imidazole. *Photochem. Photobiol.* **2016**, *92*, 546−551.
(51) Bartoloni, F. H.; de Oliveira, M. A.; Augusto, F. A.; Bastos, E. L.; Baader, W. J. Chemiluminescence Efficiency of Catalyzed 1,2-Dioxetanone Decomposition Determined by Steric Effects. *J. Org. Chem.* **2015**, *80*, 3745−3751.
(52) de Oliveira, M. A.; Augusto, F. A.; Ciscato, L. F.; Bastos, E. L.; Baader, W. J. Revision of Singlet Quantum Yields in the Catalyzed Decomposition of Cyclic Peroxides. *J. Org. Chem.* **2012**, *77*, 10537−10544.
(53) Turro, N. J. *Modern Molecular Photochemistry*; The Benjamin/Cummings Publishing Co. Inc.: Menlo Park, 1978.
(54) Aizawa, N.; Harabuchi, Y.; Maeda, S.; Pu, Y.-J. Kinetic prediction of reverse intersystem crossing in organic donor−acceptor molecules. *Nat. Commun.* **2020**, *11*, 3909.
(55) Eckersley, T. J.; Rogers, N. A. J. Photochemical studies on bicyclic $\beta\gamma$-unsaturated ketones: II[1]. Okadi-π-methane rearrangements originating from some state other than T_1 (π-π^*). *Tetrahedron* **1984**, *40*, 3759−3768.
(56) Mirbach, M. J.; Henne, A.; Schaffner, K. Rearrangement of an excited β,γ-unsaturated ketone generated by dioxetane thermolysis. On the $T_1(\pi,\pi^*)$ and $T_2(n,\pi^*)$ reactivities. *J. Am. Chem. Soc.* **1978**, *100*, 7127−7128.
(57) Zimmerman, H. E.; Keck, G. E.; Pflederer, J. L. Molecular rearrangements of excited states generated by intramolecular dioxetane scission. Photochemistry without light. Mechanistic and exploratory organic photochemistry. *J. Am. Chem. Soc.* **1976**, *98*, 5574−5581.
(58) Zimmerman, H. E.; Keck, G. E. Photochemical rearrangement without light. 95. Dioxetane effected photochemistry by direct intramolecular excitation. *J. Am. Chem. Soc.* **1975**, *97*, 3527−3528.
(59) Schramm, S.; Karothu, D. P.; Lui, N. M.; Commins, P.; Ahmed, E.; Catalano, L.; Li, L.; Weston, J.; Moriwaki, T.; Solntsev, K. M.; Naumov, P. Thermochemiluminescent Peroxide Crystals. *Nat. Commun.* **2019**, *10*, 997.
(60) Farahani, P.; Baader, W. J. Unimolecular Decomposition Mechanism of 1,2-Dioxetanedione: Concerted or Biradical? That Is the Question! *J. Phys. Chem. A* **2017**, *121*, 1189−1194.
(61) Farahani, P.; Oliveira, M. A.; Galván, I. F.; Baader, W. J. A Combined Theoretical and Experimental Study on the Mechanism of Spiro-Adamantyl-1,2-Dioxetanone Decomposition. *RSC Adv.* **2017**, *7*, 17462−17472.
(62) Bechara, E. J. H.; Wilson, T. Alkyl Substituent Effects on Dioxetane Properties. Tetraethyl-, Dicyclohexylidene-, and 3,4-Dimethyl-3,4-Di-n-Butyldioxetanes. A Discussion of Decomposition Mechanisms. *J. Org. Chem.* **1980**, *45*, 5261−5268.
(63) Adam, W. Determination of Chemiexcitation Yields in the Thermal Generation of Electronic Excitation from 1,2-Dioxetanes. *Chemical and Biological Generation of Excited States*; Adam, W., Cilento, G., Eds.; Academic Press, 1982; pp 115−152.
(64) Boaro, A.; Ageitos, L.; Torres, M.; Bartoloni, F. H.; de la Fuente-Nunez, C. Light-Emitting Probes for Labeling Peptides. *Cell Rep. Phys. Sci.* **2020**, *1*, 100257.
(65) Premi, S.; Brash, D. E. Chemical Excitation of Electrons: A Dark Path to Melanoma. *DNA Repair* **2016**, *44*, 169−177.
(66) Koo, J.-Y.; Schuster, G. B. Chemically Initiated Electron Exchange Luminescence. A New Chemiluminescent Reaction Path for Organic Peroxides. *J. Am. Chem. Soc.* **1977**, *99*, 6107−6109.
(67) Koo, J. A.; Schmidt, S. P.; Schuster, G. B. Bioluminescence of the Firefly: Key Steps in the Formation of the Electronically Excited State for Model Systems. *Proc. Natl. Acad. Sci. U.S.A.* **1978**, *75*, 30−33.
(68) Koo, J.-Y.; Schuster, G. B. Chemiluminescence of Diphenoyl Peroxide. Chemically Initiated Electron Exchange Luminescence. A New General Mechanism for Chemical Production of Electronically Excited States. *J. Am. Chem. Soc.* **1978**, *100*, 4496−4503.
(69) Schaap, A. P.; Handley, R. S.; Giri, B. P. Chemical and Enzymatic Triggering of 1,2-Dioxetanes. 1: Aryl Esterase-Catalyzed Chemiluminescence from a Naphthyl Acetate-Substituted Dioxetane. *Tetrahedron Lett.* **1987**, *28*, 935−938.
(70) Schaap, A. P.; Gagnon, S. D. Chemiluminescence from a Phenoxide-Substituted 1,2-Dioxetane: A Model for Firefly Bioluminescence. *J. Am. Chem. Soc.* **1982**, *104*, 3504−3506.
(71) Nery, A. L. P.; Röpke, S.; Catalani, L. H.; Baader, W. J. Fluoride-Triggered Decomposition of m-Sililoxyphenyl-Substituted Dioxetanes by an Intramolecular Electron Transfer (CIEEL) Mechanism. *Tetrahedron Lett.* **1999**, *40*, 2443−2446.
(72) Adam, W.; Matsumoto, M.; Trofimov, A. V. Viscosity Dependence of the Chemically Induced Electron-Exchange Chemiluminescence Triggered from a Bicyclic Dioxetane. *J. Am. Chem. Soc.* **2000**, *122*, 8631−8634.
(73) Khalid, M.; Souza, S. P., Jr.; Ciscato, L. F. M. L.; Bartoloni, F. H.; Baader, W. J. Solvent viscosity influence on the chemiexcitation efficiency of inter and intramolecular chemiluminescence systems. *Photochem. Photobiol. Sci.* **2015**, *14*, 1296−1305.
(74) Khalid, M.; de Souza, S. P., Jr.; Bartoloni, F. H.; Augusto, F. A.; Baader, W. J. Chemiexcitation Efficiency of Intermolecular Electron-transfer Catalyzed Peroxide Decomposition Shows Low Sensitivity to Solvent-cavity. *Photochem. Photobiol.* **2016**, *92*, 537−545.
(75) Catalani, L. H.; Wilson, T. Electron transfer and chemiluminescence. Two inefficient systems: 1,4-dimethoxy-9,10-diphenylanthracene peroxide and diphenoyl peroxide. *J. Am. Chem. Soc.* **1989**, *111*, 2633−2639.
(76) Isobe, H.; Takano, Y.; Okumura, M.; Kuramitsu, S.; Yamaguchi, K. Mechanistic insights in charge-transfer-induced luminescence of 1,2-dioxetanones with a substituent of low oxidation potential. *J. Am. Chem. Soc.* **2005**, *127*, 8667−8679.
(77) Takano, Y.; Tsunesada, T.; Isobe, H.; Yoshioka, Y.; Yamaguchi, K.; Saito, I. Theoretical studies of decomposition reactions of dioxetane, dioxetanone, and related species. CT induced luminescence mechanism revisited. *Bull. Chem. Soc. Jpn.* **1999**, *72*, 213−225.
(78) da Silva, L. P.; Pereira, R. F. J.; Magalhães, C. M.; Silva, J. C. G. E. Mechanistic Insight into Cypridina Bioluminescence with a Combined Experimental and Theoretical Chemiluminescent Approach. *J. Phys. Chem. B* **2017**, *121*, 7862−7871.
(79) Magalhães, C. M.; da Silva, J. C. G. E.; da Silva, L. P. Study of coelenterazine luminescence: Electrostatic interactions as the controlling factor for efficient chemiexcitation. *J. Lumin.* **2018**, *199*, 339−347.
(80) Silva, L. P.; Magalhães, C. M. Mechanistic insights into the efficient intramolecular chemiexcitation of dioxetanones from TD-DFT and multireference calculations. *Int. J. Quantum Chem.* **2018**, *119*, No. e25881.
(81) Cotton, M. L.; Dunford, H. B. Studies on Horseradish Peroxidase. XI. On the Nature of Compounds I and II as Determined from the Kinetics of the Oxidation of Ferrocyanide. *Can. J. Chem.* **1973**, *51*, 582−587.

https://doi.org/10.1021/acs.joc.1c00230
J. Org. Chem. 2021, 86, 6633−6647